

3-2015

Hybrid Electric Power System Validation through Parameter Optimization

Hasnaa Khalifi

Follow this and additional works at: <https://commons.erau.edu/edt>



Part of the [Electrical and Computer Engineering Commons](#)

Scholarly Commons Citation

Khalifi, Hasnaa, "Hybrid Electric Power System Validation through Parameter Optimization" (2015).
Dissertations and Theses. 220.

<https://commons.erau.edu/edt/220>

This Thesis - Open Access is brought to you for free and open access by Scholarly Commons. It has been accepted for inclusion in Dissertations and Theses by an authorized administrator of Scholarly Commons. For more information, please contact commons@erau.edu.

Hybrid Electric Power System Validation through Parameter Optimization

by

Hasnaa Khalifi

A Thesis Submitted to the College of Engineering Department of Mechanical
Engineering in Partial Fulfillment of the Requirements for the Degree of
Master of Science in Mechanical Engineering

Embry-Riddle Aeronautical University
Daytona Beach, Florida
March 2015

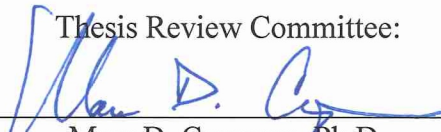
Hybrid Electric Power System Validation Through Parameter Optimization

by

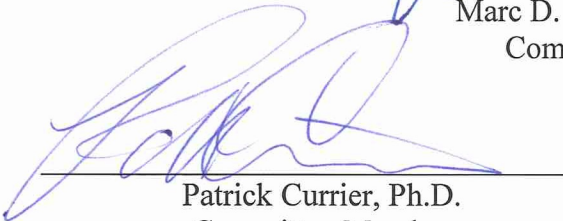
Hasnaa Khalifi

This thesis was prepared under the direction of the candidate's Thesis Committee Chair, Dr. Marc D. Compere, Associate Professor, Daytona Beach Campus, and Thesis Committee Members Dr. Patrick Currier, Assistant Professor, Daytona Beach Campus, and Dr. Ilteris Demirkiran, Professor, Daytona Beach Campus, and has been approved by the Thesis Committee. It was submitted to the Department of Mechanical Engineering in partial fulfillment of the requirements for the degree of Master of Science in Mechanical Engineering

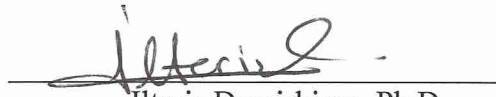
Thesis Review Committee:



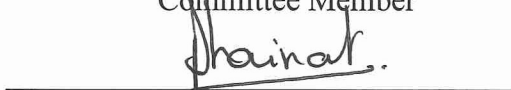
Marc D. Compere, Ph.D.
Committee Chair



Patrick Currier, Ph.D.
Committee Member



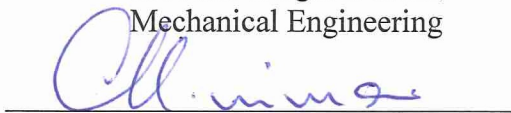
Ilteris Demirkiran, Ph.D.
Committee Member



Jean-Michel M. Dhainaut, Ph.D.
Graduate Program Chair,
Mechanical Engineering



Charles F. Reinholtz, Ph.D.
Department Chair,
Mechanical Engineering



Maj Mirmirani, Ph.D.
Dean, College of Engineering



Robert Oxley, Ph.D.
Associate Vice President of Academics

4-9-2015
Date

Acknowledgements

First and foremost, I would like to thank my parents for their unconditional love and support. They always have been a major inspiration in my life and I dedicate this thesis to them.

I would like to express my deep gratitude to my advisor Dr. Marc Compere for his guidance and encouragements. I first met Dr. Compere through the hybrid and electric vehicle class in the fall of 2013, since then, he has been a major inspiration in my career and I could not imagine having a better mentor.

I would like to thank Dr. Patrick Currier for his insightful research advice, for making it possible to be part of the EcoCar program and for allowing me to conduct tests at the EcoCar Lab.

I would like to thank Dr. Ilteris Demirkiran for his encouragements and for being part of my thesis committee.

I would like to thank the EcoCar team for helping me conduct vehicle tests and providing me with additional data to validate.

Finally, I would like to thank Argonne National Lab, General Motors, and the US Department of Energy for organizing and supporting the EcoCAR2: Plugging Into the Future program.

Abstract

Researcher: Hasnaa Khalifi

Title: Hybrid Electric Power System Validation Through Parameter Optimization

Institution: Embry-Riddle Aeronautical University

Degree: Master of Science in Mechanical Engineering

Year: 2015

Battery models can be developed from first principles or from empirical methods. The work presented in this thesis is semi-empirical, the model was validated using test data through parameter optimization. Simulink Parameter Estimation toolbox was used to identify the battery parameters and validate the battery model with test data. Experimental data was obtained by discharging the battery of a modified 2013 Chevrolet Malibu hybrid electric vehicle. The resulting battery model provided accurate simulation results over the validation data. For the constant current discharge, the mean squared error between measured and simulated data was 0.26 volts for the terminal voltage, and $6.07e-4$ (%) for state of charge. For the extended variable current discharge, the mean squared error between measured and simulated data was 0.21 volts for terminal voltage and $9.25e-4$ (%) for state of charge. The validated battery model was implemented in the hybrid electric vehicle model and an optimization routine was conducted in Simulink to validate a launch control strategy. The vehicle model was subject to two maximum acceleration tests from 0-60mph. Test 1 corresponded to a maximum acceleration in EV-only mode and test 2 corresponded to a maximum acceleration in HEV mode or launch control mode. In both tests, the simulated data matched the experimental data with a root mean square error below 0.45 mph for vehicle speed and 3.5 volts for bus voltage.

Table of Contents

	Page
Thesis Review Committee	ii
Acknowledgements.....	iii
Abstract	iv
List of Tables	vii
List of Figures	viii
Chapter	
I Introduction.....	1
Background and Motivation	1
Physical System	3
Optimization	4
Thesis Statement	5
Organization.....	5
List of Acronyms	6
II Review of the Relevant Literature	7
Optimization Methods for Model Validation	7
Battery Modeling and Parameter Estimation	9
HEV Power System Model Validation	11
III Methodology	13
Parameter Identification	13
Simulink Approach to Parameter Identification	14
Simulink Implementation.....	15

	Trust-Region Reflective Algorithm	17
	Model Development.....	17
	Battery Model	18
	ESS Parameter Estimation Process.....	22
	Vehicle Power System Model.....	25
	Experimental Apparatus.....	30
	Battery Test Procedure.....	30
	Maximum Acceleration 0-60mph Vehicle Tests	31
IV	Results.....	33
	Battery Model	33
	Vehicle Model 0-60mph Acceleration Tests	39
V	Discussion, Conclusions, and Recommendations.....	48
	Parameter Optimization Theory.....	48
	ESS Parameter Optimization	48
	Vehicle Parameter Optimization.....	48
	Recommendations.....	49
Appendices		
A	Bibliography	51
B	Simulink Optimization Toolbox	54
C	Battery Simulink Model.....	55

List of Tables

Table 1: Battery specifications.....	21
Table 2: Estimated battery parameters using Simulink Design Optimization.....	35
Table 3. Estimated Vehicle parameters using Simulink 2014a Optimization toolbox	40

List of Figures

Figure 1: Model Validation Process Flow Diagram	2
Figure 2: Embry-Riddle EcoCAR 2 Diesel Series PHEV	5
Figure 3: A simple battery model	9
Figure 4: Thevenin battery model.....	10
Figure 5: Parameter estimation strategy using Simulink	14
Figure 6: Measured data Y versus simulated data \hat{Y} showing the residual ri	16
Figure 7: Circuit diagram of the battery model	18
Figure 8: Battery Simulink model showing the inputs and outputs.....	19
Figure 9: Simulink Parameter Estimation Process.....	22
Figure 10: Data Import in Simulink 2014a Parameter Estimation Toolbox.....	23
Figure 11: Variables designation in Simulink 2014a Parameter Estimation Toolbox.....	24
Figure 12: Estimation Routine in Simulink 2014a Parameter Estimation Toolbox	25
Figure 13: High Voltage Power System Components [22]	26
Figure 14: Remy HVH250-090P torque as a function of DC bus voltage	27
Figure 15: Simulink motor model provides torque as a function of	27
Figure 16: Engine Simulink model showing engine speed as a.....	29
Figure 17: Vehicle on dynamometer drum	31
Figure 18. Parameter trajectories showing convergence	34
Figure 19: Measured and simulated voltage for a discharge current of 100 Amps	36
Figure 20: Measured and simulated SOC for a discharge current of 100 Amps	37
Figure 21: Measured and simulated voltage for a variable discharge current	38
Figure 22: Measured and simulated SOC for a variable discharge current	39

Figure 23: Maximum Acceleration from 0-60mph validation in EV-mode	41
Figure 24: Maximum Acceleration from 0-60mph validation in HEV-mode	42
Figure 25: Bus Voltage validation in EV- mode	43
Figure 26: Bus Voltage validation in HEV- mode.....	43
Figure 27: Measured and simulated battery current in EV-mode.....	44
Figure 28: Measured and simulated battery and Generator current in HEV-mode	45
Figure 29: Measured and simulated traction motor torque in EV-mode	46
Figure 30: Measured and simulated traction motor torque in HEV-mode	46

Chapter I

Introduction

1.1 Background and Motivation

The EcoCAR 2 program is an advanced vehicle competition challenging 15 schools from the United States and Canada to design and implement the most efficient hybrid electric vehicle architecture. It is run by Argonne National Lab and sponsored by General Motors and the United States department of Energy [1]. The program completed years 1, 2, and 3. Year 1 focused on design and simulation of the hybrid vehicle. Year 2 focused on design integration and assembly. During year 3, the vehicle provided an ideal research platform for data collection and experimentation at the component and system level. Increased use of hybrid electric vehicles reduces fuel consumption, greenhouse gases and other regulated emissions. The studied vehicle was a modified 2013 Chevrolet Malibu hybrid electric vehicle.

This thesis presents experimental data collection, physical system modeling, and optimization methods for the energy storage system (ESS) and vehicle's 0-60mph acceleration tests. This work is motivated by a need to validate physical system models with the hardware's experimental data. Figure 1 shows an example model validation process flow diagram. Another goal of this thesis is to provide EcoCAR 3 with an ESS model to implement in the vehicle power system model. ESS physical system modeling allows to evaluate and predict the performance of battery operated electric power systems. It can be developed from first principles or empirical methods.

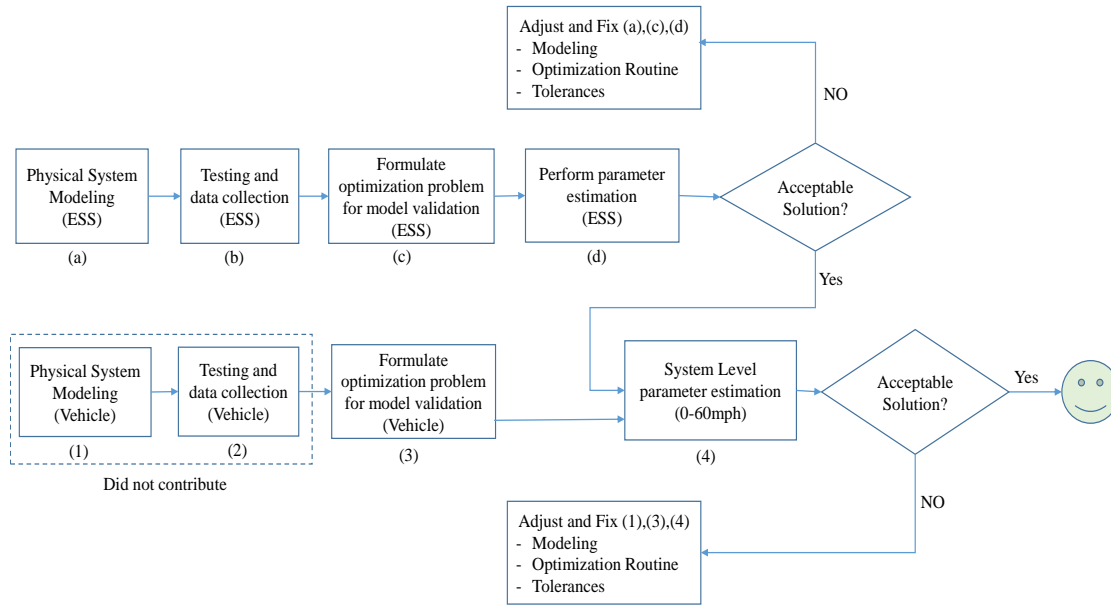


Figure 1: Model Validation Process Flow Diagram

The main contribution of this thesis is shown in Figure 1. First, an ESS model for the hybrid electric vehicle was developed. With the help of the EcoCAR team, chassis dynamometer testing were conducted in order to collect discharge battery data. The optimization problem for model validation was formulated. Once the battery model was validated, it was implemented in a physical system model of the vehicle. Finally, system level parameter estimation was conducted in order to validate a launch control strategy. The contribution does not include vehicle system level modeling nor to the vehicle maximum acceleration testing and data collection.

1.2 Physical System

Hybrid electric vehicles combine the advantages of a combustion engine, an electric motor and the energy storage system (ESS) to obtain improved fuel economy, reduced emissions and increased power output.

Hybrid electric vehicles have the advantage of operating in different modes. At low speeds, the vehicle may be propelled solely from the ESS; this is called pure electric traction mode. When the ESS is depleted, the vehicle is set to pure engine traction mode, where the engine or generator supplies the traction power. The vehicle may also operate in hybrid traction mode where the engine generator and the ESS supply the tractive power. During regenerative braking mode, the traction motor operates as a generator powered by the vehicle's kinetic or potential energy; the power generated charges the ESS [2].

The three most common hybrid vehicle architectures are series hybrid, parallel hybrid and series-parallel hybrid. A series hybrid drive train combines the power from the engine generator and electric machine to propel the vehicle. The electric motor is the only means to power the wheels. A parallel hybrid uses the power from the internal combustion engine (ICE) and the electric machine individually or in combination to propel the vehicle. The electric motor and the ICE are mechanically coupled to the wheels [3]. A series-parallel hybrid combines the advantages of the series and parallel configurations at some cost in complexity. It employs two power couplers: mechanical and electrical [2].

Rechargeable batteries are an essential part of a hybrid electrical vehicle. When the vehicle is operating on electric mode only, the total vehicle emissions are reduced and the

energy efficiency is increased. This reduces petroleum consumption and the vehicle's operating costs [4].

Battery models play a significant role in evaluating and predicting the performance of battery operated electric power systems. Increased use of electric vehicles reduces fuel consumption, greenhouse gasses and other regulated emissions. Battery models can be developed from first principles or from empirical methods.

1.3 Optimization

Model validation using parameter optimization is an essential tool to accurately predict the behavior of dynamic systems [5]. The key parameters for hybrid electric vehicle power systems are usually found in manufacturer datasheets. These values are not always accurate or complete. Datasheets usually provide the rated values under specific conditions, which are not always representative of the power system behavior during a drive cycle. Parameter optimization can be conducted through the Simulink optimization toolbox for component or system level validation. It uses experimental data and state-of-the-art optimization methods to compute the model parameters [6]. This eliminates the need to change parameters by hand through trial and error or develop a complex parameter optimization routine especially when there is a large number of unknown parameters. The Simulink optimization toolbox is also able to optimize multiple model outputs of equal or different quality. Weight factors, w_j may be specified for each output depending on the degree of importance.

Thesis Statement

A Lithium-Ion battery model was developed and validated for Embry-Riddle EcoCAR2 Diesel Series plugin hybrid electric vehicle. Chassis dynamometer testing was performed and the data used for component validation of the battery. The validated ESS model was integrated into a hybrid vehicle power system model. Parameter optimization was then used to estimate uncertain system level model parameters to validate vehicle performance with high acceleration test data.

Organization

Chapter 1 presents the introduction, which includes the background, motivation and the thesis statement. Chapter 2 presents the literature review on parameter optimization for model validation and hybrid electric vehicle battery modeling. Chapter 3 presents the methodology for optimization and vehicle component modeling. Chapter 4 presents the validated model results compared to the measured data. Chapter 5 presents the discussions, conclusions and recommendations.



Figure 2: Embry-Riddle EcoCAR 2 Diesel Series PHEV

List of Acronyms

PHEV	plugin hybrid electric vehicle
EV	Electric Vehicle
HEV	Hybrid Electric Vehicle
ESS	Energy Storage System
ICE	Internal Combustion Engine
SOC	State of Charge
SSE	The Sum of the Square of the Errors
OCV	Open Circuit Voltage
SCU	Supervisory Control Unit

Chapter II

Review of the Relevant Literature

This chapter presents a critical literature review of optimization methods for model validation, battery modeling methods, and hybrid power system model validation.

Section 2.1 reviews theory for using parameter optimization during model validation.

Section 2.2 provides a complete example of model validation at the component level with test data for a hybrid battery system. Section 2.3 provides a second example of model validation for system-level validation for a complete vehicle.

2.1 Optimization Methods for Model Validation

The primary goal of optimization is to minimize a cost function under constraints. In Simulink parameter estimation, the cost function is the error between the simulated and measured output. Multiple optimization methods and algorithms are available to choose from. The default optimization method is the nonlinear least square method which minimizes the cost function by changing the parameter values [7].

Simulink Design Optimization toolbox can be used to calibrate the model data, by modifying key parameters, in order to match the measured output. In Simulink, this is called parameter estimation. The toolbox also comprises of other optimization options such as response optimization. It optimizes the model response to satisfy design requirement and system robustness. A sensitivity analysis can be conducted to analyze how parameters and states of a model affect the cost function; these parameters can be ranked in order of influence [8]. The optimization method and algorithm can be specified in the parameter estimation toolbox. Some of the available optimization methods are the Gauss-newton Method and the gradient Descent Method.

Gauss-Newton is a basic method for optimization and consists of forward, backward or central differential numerical derivative, shown respectively in (9).

$$\begin{aligned}\frac{dy}{dx} &= \frac{y(x + \Delta x) - y(x)}{\Delta x} \\ \frac{dy}{dx} &= \frac{y(x) - y(x + \Delta x)}{\Delta x} \\ \frac{dy}{dx} &= \frac{y(x + \Delta x) - y(x - \Delta x)}{2\Delta x}\end{aligned}\tag{9}$$

Another Simulink optimization method is the Gradient Descent [9]. It uses *fmincon* function to optimize the response signal subject to constraints. Its default algorithm is the Sequential Quadratic Programming (sqp). The sqp algorithm uses sets of linear algebra routines to solve the optimization problem. It takes iterative steps in the constrained region, the steps respect the constrained bounds and can be as far as exactly on the boundary.

A Mathworks article [10] describes a workflow for creating a high-fidelity model of an electric motor using Matlab and Simulink. Model parameters were identified from test data and verified through simulation using Simulink Design Optimization toolbox. Parameter values were verified by comparing simulation results with measured data. It was found that the simulation matched the hardware results with a normalized mean square deviation below 2% for key signals such as rotor velocity and motor phase currents.

Advanced optimal control textbooks [11-13] discuss the optimization problem as an estimator or ‘observer’ and it is cast within a control theoretic framework. An observer is used in control system design to take live signal inputs and generate a model online, in

real-time, which is useful for control purposes. The parameter estimation conducted in this thesis is offline, and assumes full signal availability for offline use and recall.

2.2 Battery Modeling and Parameter Estimation

The two most common battery models are the electrochemical models and the electric circuit models. The electrochemical models are based on chemical reactions inside the battery. They are the most accurate because of their ability to simulate the cells at a molecular level. Electrochemical simulations may take hours or days of time and therefore are not the best candidates for system level simulations. The electrical circuit models are the most commonly used for electrical and electro-mechanical engineering simulations because of their electrical nature and the straight forward interface to other electrical component [14].

The simplest battery model consists of one constant internal resistance in series with a voltage source, as shown in Figure 3. While this model is popular because of its simplicity, it does not take into consideration the variation of the internal impedance of the battery with the varying SOC. This model is best used in simulations where the energy drawn out of the battery is assumed to be infinite and the SOC is of little importance. It would not be appropriate for hybrid and electric vehicle simulations [15].

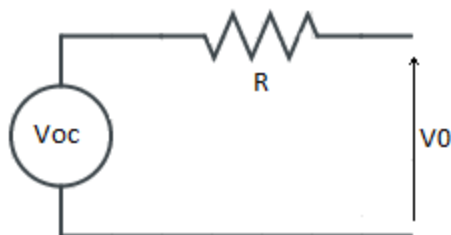


Figure 3: A simple battery model

Another commonly used battery model is the Thevenin equivalent circuit model [16]. The Thevenin model uses an open circuit voltage in series with a resistor and a parallel RC block to track the battery response to transient loads [17]. Increasing the number of parallel RC blocks may increase the accuracy of the model.

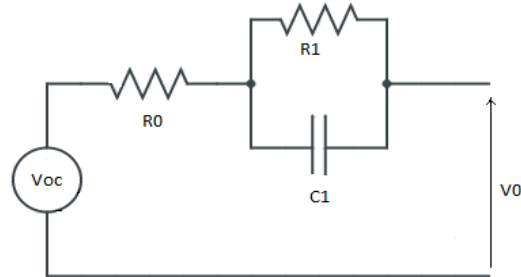


Figure 4: Thevenin battery model

A lead acid battery equivalent circuit model was analyzed in [18]. It consists of n RC-blocks connected in series with a terminal resistance and a voltage source, where n is a positive number. The authors present the dynamic equations for the model and describe in detail the parameter identification procedure by using lab tests data and manufacturer's data.

Similarly, [19] uses an electrical circuit consisting of one RC branch in series with a resistance to model a lead acid battery. The battery's outputs were a function of state of charge and temperature. The model uses the same dynamic equations of [18]. The battery parameters were estimated from laboratory data using the Simulink optimization toolbox.

An equivalent circuit model for a Lithium (LiNiCoMnO₂) battery, consisting of one voltage source, one series resistor, and a single RC block was presented in [20]. The parameter estimation used pulse current discharge tests on lithium cells and showed

circuit elements dependence on SOC, average current and temperature. For Lithium cells, the most common equivalent circuit consists of one or two RC. The parameter estimation was run for a range of discharge experiments at different temperatures. The results provided 2D lookup tables for each of the four circuit elements: $R_0 = R_0(SOC, T)$, $R_1 = R_1(SOC, T)$, $V_{oc} = V_{oc}(SOC, T)$. In the experimental setup, Lithium ion cells were tested at three different temperatures: 5C, 20C and 40C. The cell was initially charged and then subjected to partial discharge-rest phase cycles. The voltage at the end of each one-hour rest period was stable enough to be considered as a good estimate for OCV. SOC was derived using Coulomb counting of the current drawn at each step [20]. For the parameter estimation, each temperature was considered independent.

A three RC model was chosen for the battery in [21]. Increasing the number of RC branches, causes increased parameter estimation complexity. The authors propose a way to solve the complex parameter estimation by reducing the size of the problem and breaking the data using a layered approach. The data was split into separate estimation tasks for each pulse or SOC level. In task 1, all the data exercised the 100% and 99% SOC breakpoints. These two columns were optimized only in Task1. After Task1 was complete, the exact SOC was recorded at the location where Task 2 starts. Task 2 began when the battery was near steady state right before the second pulse. The authors also presents a step by step parameter estimation procedure for the 3 RC branch configuration.

2.3 Hybrid Electric Power System Model Validation

A launch control strategy for improving maximum acceleration in a series hybrid electric vehicle is presented in [20]. The tested vehicle is a modified 2013 Chevrolet Malibu. The vehicle was accelerated from 0-60mph and tested under two power system

modes: EV-only mode (test 1) and HEV performance mode (test 2). In test 1, the ESS was the sole source of power and mobility, the driver applied maximum throttle until the vehicle slightly exceeded 60mph. In test 2, the driver engaged launch control mode by pressing a dashboard button, shifting into neutral, applying full throttle and then shifting the lever from neutral to drive; this allowed the engine-generator to enter charge sustaining mode. Both tests were performed on the same road, in the same direction and with the same driver and passenger to ensure uniformity. The experimental data shows that the HEV mode presents a 0.59 sec time reduction compared to the EV-only mode. This is primarily due to the engine generator's additional power supply to the high voltage DC bus and the ability to apply maximum torque quickly.

This thesis validates the systems level vehicle model against measured hardware test data in [22]. Simulink optimization toolbox was used to identify key parameters for the vehicle model.

Chapter III

Methodology

This chapter presents the parameter identification theory and methods using Simulink Parameter Estimation toolbox. It also presents the procedures for battery and vehicle power system modeling.

Simulink Parameter Estimation toolbox was used to identify the battery parameters and validate the battery model. Experimental data was obtained by discharging the battery of a modified 2013 Chevrolet Malibu hybrid electric vehicle. The validated battery model was implemented in the hybrid electric vehicle model and an optimization was conducted in Simulink to validate a launch control strategy.

3.1 Parameter Identification

The objective of the offline parameter optimization problem is to minimize a cost function J by finding the design parameter b subject to differential constraint \dot{x} , equality constraint c , and inequality constraint d to produce the output y [11],

$$\begin{aligned}\dot{x} &= f(x, t, u, b), \\ c(x) &= 0, \\ d(x) &\geq 0, \\ y &= h(x, t, b).\end{aligned}\tag{1}$$

The cost function is defined as,

$$J = \sum_{i=1}^n w_j (y_i - \hat{y}_i)^2\tag{2}$$

where w_j is a weight factor, y_i is the experimental data and \hat{y}_i is the modeled data. The subscript i denotes the time series for the j^{th} measured signal. The parameters b_i are changed until the stopping criterion is reached: if two successive parameter or function values change by less than the chosen parameter or function tolerance, $|b_{i+1} - b_i| < \varepsilon_1$ or $|J_{i+1} - J_i| < \varepsilon_2$, respectively or when the maximum number of iterations is reached.

3.2 Simulink Approach to Parameter Identification

In Simulink Parameter Estimation, the simulation uses an iterative approach, it runs from $[0 - t_f]$ and the model parameters are found such that the modeling error r_i is minimized.

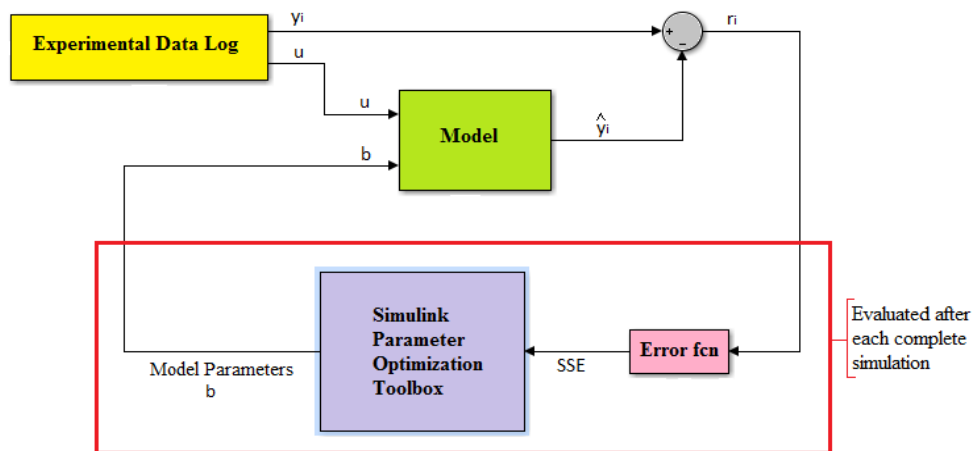


Figure 5: Parameter estimation strategy using Simulink

Simulink parameter estimation toolbox was used to determine key parameters to match the simulation results with the measured data. First, the desired output signal was specified as an output in Simulink before running the simulation then the test data signal was imported into the parameter estimation toolbox. The model parameters and initial

conditions were selected and finally the estimation method and algorithm options were specified to define the optimization. The optimization stopping criterion is decided by a number of factors: if two successive parameter or function values change by less the chosen parameter or function tolerance, $|b_{i+1} - b_i| < \varepsilon_1$ or $|J_{i+1} - J_i| < \varepsilon_2$, respectively, or if the maximum number of iterations is reached. By modifying these parameters, the optimization can continue searching for a more accurate solution.

Other sources of error in the parameter optimization process include the error associated with the numerical integration such as a fixed step search versus a variable step and the solver order. The optimization routine termination based on parameter or function tolerances and the interpolation error caused by the experimental data and output data comprising of different numbers of data points.

3.3 Simulink Implementation

In Simulink Parameter Estimation [23], the default estimation method is the nonlinear least square. It uses the nonlinear least squares function *lsqnonlin* and its algorithm options are the Trust-Region-Reflective Least Squares Algorithm (default) or the Levenberg-Marquardt Method. The optimization method used in this work is the nonlinear least square with the Trust-Region-Reflective algorithm.

The least square method minimizes the sum square of residuals when estimating parameters. Consider an i^{th} data point with a residual r_i ,

$$r_i = y_i - \hat{y}_i \quad (3)$$

where y_i is the experimental data and \hat{y}_i is the modeled data, as shown in Figure 6. The sum of the square of the residuals is given by,

$$SSE = J = \sum_{i=1}^n r_i = \sum_{i=1}^n w_j (y_i - \hat{y}_i)^2 \quad (4)$$

where n is the number of data points. When parameter estimation depends on the optimization of multiple data sets of unequal certainty, a weight scale factor w_j can be used to bias the error presented to the solver.

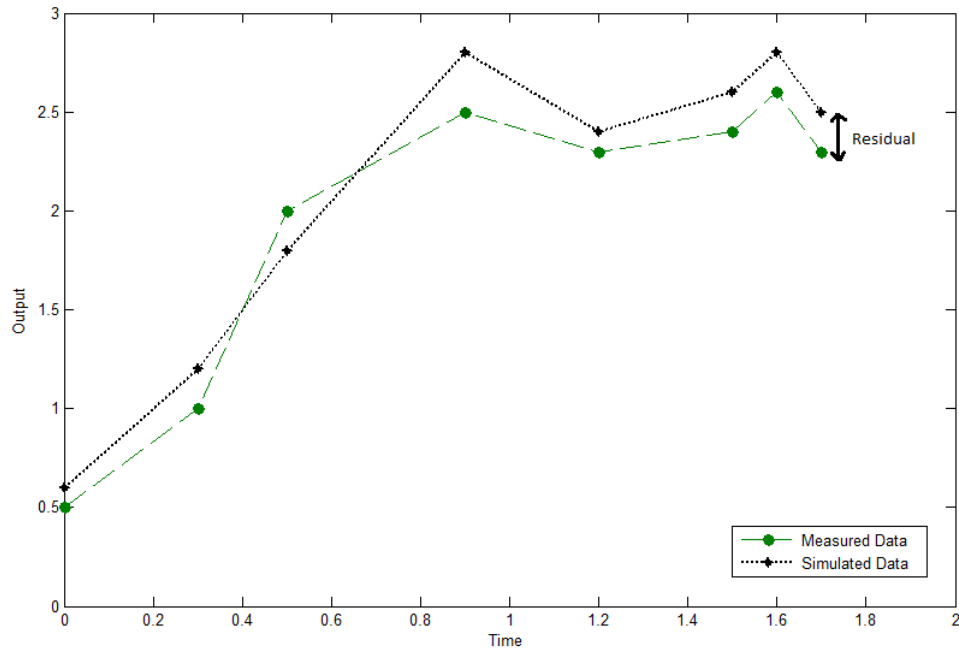


Figure 6: Measured data Y versus simulated data \hat{Y} showing the residual r_i

The nonlinear least square method fits a nonlinear model to the data and has nonlinear parameters or a combination of linear and nonlinear parameters. It has the form,

$$y = f(X, b) + \varepsilon \quad (5)$$

where y is the response vector, f is a function of the parameter vector b and a predictor variable matrix X treated as coefficients and ε is the errors vector. The nonlinear approach starts with initial estimates for each parameter and creates a fitted curve \hat{y} for the available sets of parameters, where $\hat{y} = f(X, b)$. Then a Jacobian calculation of $f(X, b)$ is performed. The Jacobian matrix is defined as the partial derivative of cost function $J = \phi(x)$ with respect to x ,

$$Jacobian = \phi_x = \frac{\partial \phi}{\partial x} = \begin{pmatrix} \frac{\partial \phi_1}{\partial x_1} & \dots & \frac{\partial \phi_1}{\partial x_n} \\ \vdots & \ddots & \vdots \\ \frac{\partial \phi_n}{\partial x_1} & \dots & \frac{\partial \phi_n}{\partial x_n} \end{pmatrix} \quad (6)$$

Simulink evaluates the Jacobian numerically. The parameters are adjusted to improve the fit based on the fitting algorithm.

3.3.1. Trust-Region Reflective Algorithm

The default algorithm is the Trust-Region-Reflective, unlike the Levenberg-Marquardt algorithm, the parameter constraints must be specified [23]. The trust region reflective algorithm approximates the model in a region near the iterate. This region is called the trust region and is updated for each iteration. For example, suppose there is a point x_i in an n -space and we want to move to a point with a lower function value than the current point x_i , the function can be approximated by a quadratic, from its Taylor Expansion around x_i , in the neighborhood N around x_i . The improved point x_{i+1} is also in this region. The trial step $s_i = x_{i+1} - x_i$ is found by minimizing over N . The

neighborhood N is usually spherical or ellipsoidal in shape. The problem statement is as follows,

$$\min \{q(s), s \in N\}, \quad (7)$$

where,

$$q(s) = \frac{1}{2} s^T H s + s^T g \quad \text{such that } \|Ds\| \leq \Delta \quad (8)$$

where g is the gradient evaluated at x_i , H is the Hessian matrix defined as the symmetric matrix of second derivatives, D is the scaling matrix and Δ is a positive trust region size. The trust reflective region algorithm is more efficient in solving nonlinear problems compared to other algorithms such as Levenberg-Marquardt or Gauss Newton [24].

3.2 Model Development

This section presents the modeled circuit for the battery along with a vehicle subsystem description and empirical equations.

3.2.1 Battery Model

The equivalent battery model chosen for a 16kW-hr lithium iron phosphate battery consists of one RC-block connected in series with a terminal resistance and a voltage source, as shown in Figure 7.

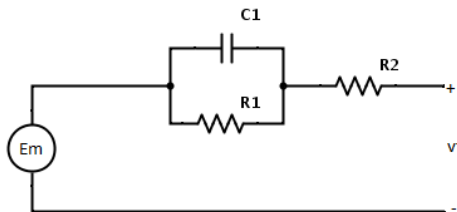


Figure 7: Circuit diagram of the battery model

In the circuit above, E_m represents the open circuit voltage, the resistance R_1 represents the branch resistance, the capacitance C_1 represents the time delay in the branch and R_2 represents the resistance at the battery terminals. The battery was modeled in Simulink. The model input is current and the outputs are voltage and state of charge, as shown in Figure 8.

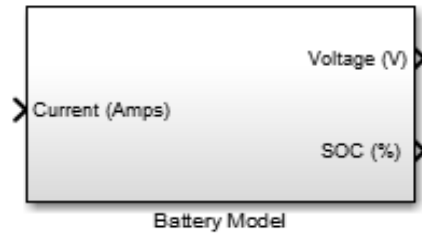


Figure 8: Battery Simulink model showing the inputs and outputs

The open circuit voltage E_m , resistances R_1 and R_2 and total capacity varied with the state of charge and temperature. The input current was divided by three, which is the number of cells in parallel, in order to model the characteristics of one cell. The output voltage was multiplied by ninety, which is the number of cells in series, in order to model the characteristics of the Chevrolet Malibu's battery pack. Equations (10) to (16) describe the modeled circuit.

The open circuit voltage is found from equation (10), where E_{m0} is the open circuit voltage in volts at full charge, T is the electrolyte temperature in $^{\circ}\text{C}$, SOC is the state of charge and K_E a constant in volts/ $^{\circ}\text{C}$.

$$E_m = E_{m0} - K_E(273 + T)(1 - SOC) \quad (10)$$

The resistance R_1 is a function of state of charge and a constant R_{10} in ohms.

$$R_1 = -R_{10} \ln(SOC) \quad (11)$$

The Capacitance C_1 is a function of the resistance R_1 in ohms and a time delay tau in seconds.

$$C_1 = \tau/R_1 \quad (12)$$

The terminal resistance R_2 is a function of state of charge and constants R_{00} in ohms and A.

$$R_2 = R_{00}[1 + A_0(1 - SOC)] \quad (13)$$

The battery's total capacity is calculated from the discharge current I in Amps, the electrolyte temperature in °C, the battery's nominal current I^* in Amps, the no-load capacity C_0 in Amp-seconds and constants K_c and δ .

$$C(I, T) = \frac{K_c C_0 K_t}{1+(K_c-1)(I/I^*)^\delta} \quad (14)$$

The state of charge measures the remaining charge in the battery, ranging from 0 to 100%. It is a function of the battery's charge in Amp-seconds and battery's capacity in Amps-seconds.

$$SOC = 1 - \frac{Q_e}{c(0,T)} \quad (15)$$

The battery's extracted charge Q_e is an integration of the current flowing through at time t .

$$Q_e(t) = Q_{e_init} + \int_0^t -I(t)dt \quad (16)$$

The battery's electrolyte temperature can be computed by solving the heat equation of a homogeneous body exchanging heat with the environment. The battery's thermal parameters are: the internal resistive losses estimated from $P_s = I^2R$, the ambient temperature, the battery's thermal resistance R_T in °C/Watts and the battery's thermal capacitance in Joules/ °C.

$$T(t) = T_{init} + \int_0^t \frac{P_s - \frac{(T-T_a)}{R_T}}{c_T} dt \quad (17)$$

The evaluated battery characteristics are shown in Table 1.

Table 1: Battery specifications

Characteristic	Value
Battery Chemistry	Lithium Iron Phosphate
Battery Pack	6 x 15s 3p
Cell Capacity (minimum)	19.6 Amp-hr
Cell Voltage (nominal)	3.24 volts
Pack Voltage (nominal)	292 volts
Pack Energy (minimum)	16.2 kW-hr
Operating Temperatures	-30°C - 60°C

3.2.2 ESS Parameter Estimation Process

The ESS model was developed in Matlab and Simulink using (10-16). Parameter optimization was conducted using Simulink Parameter Estimation Toolbox in order to validate model output with experimental data. The experimental discharge current data was input to the Simulink model and the calculated bus voltage was compared with the experimental bus voltage, as shown in Figure 9. In Simulink Parameter Estimation Toolbox, the sum of squared errors for measured and simulated voltage is calculated, the uncertain model parameters are changed until the stopping criterion is reached.

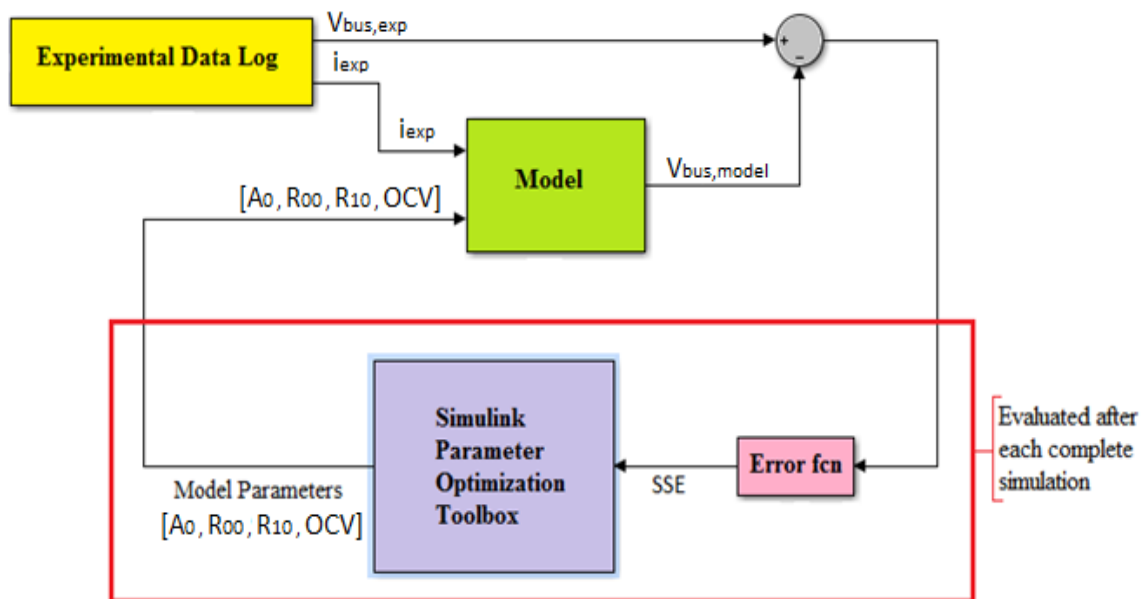


Figure 9: Simulink Parameter Estimation Process

It was necessary to specify the voltage as the highest level output in Simulink in order to appear in the parameter estimation dialog box. Under the Analysis tab in

Simulink 2014a, parameter estimation option was chosen and the voltage experimental data was imported under Transient Data as shown in Figure 10.

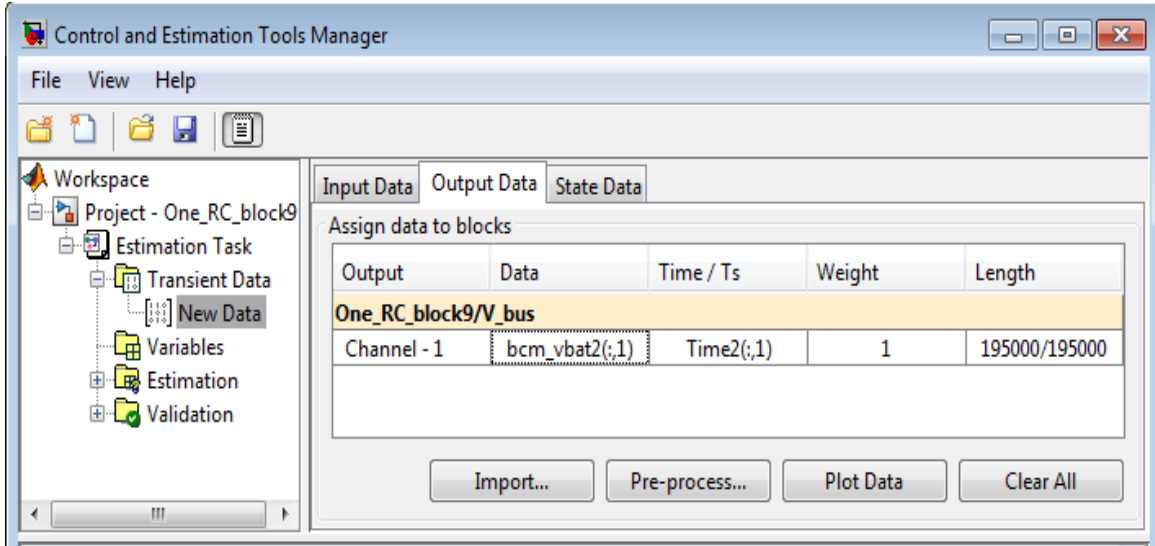


Figure 10: Data Import in Simulink 2014a Parameter Estimation Toolbox

The estimated variables were R_{00} and A_0 in (13), R_{10} in (11) and the open circuit voltage OCV which is a lookup table in Simulink varying with the state of charge. The parameters initial guess and constraints were specified under variables default settings as shown in Figure 11.

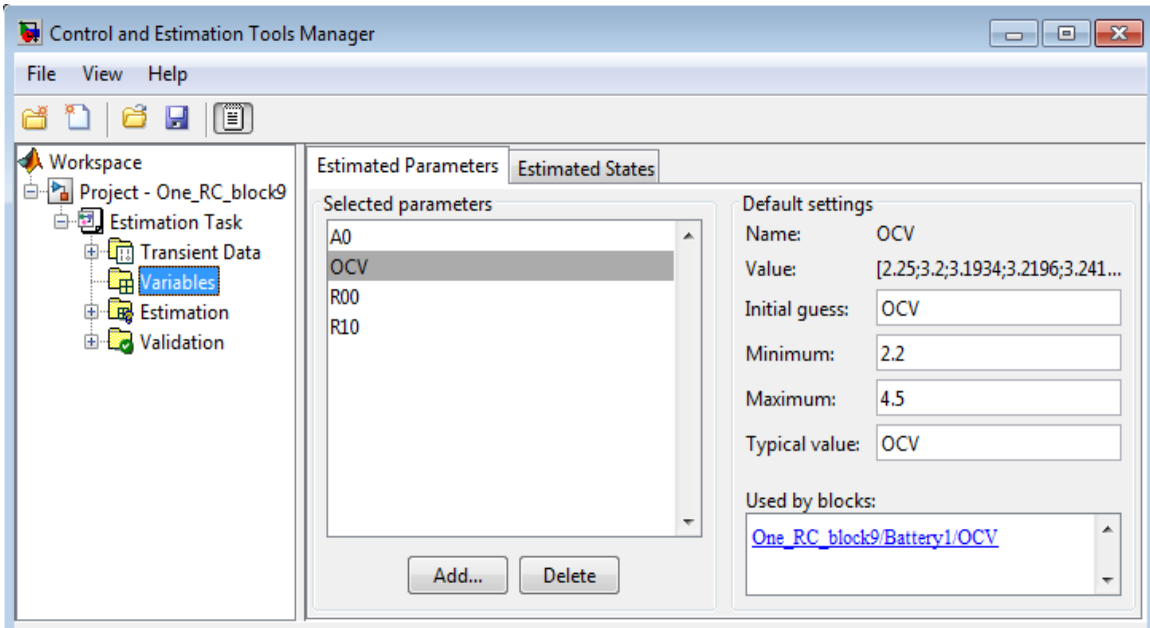


Figure 11: Variables designation in Simulink 2014a Parameter Estimation Toolbox

The optimization routine and tolerances were specified under Estimation Options, as shown in Figure 12. The method used was the nonlinear least squares with the Trust-Region-Reflective Algorithm. The parameter and function tolerances were both chosen to be $1e^{-4}$, the maximum number of function evaluations was chosen to be 700 and the maximum number of iterations was chosen to be 100. The function is evaluated 700 times for every iteration.

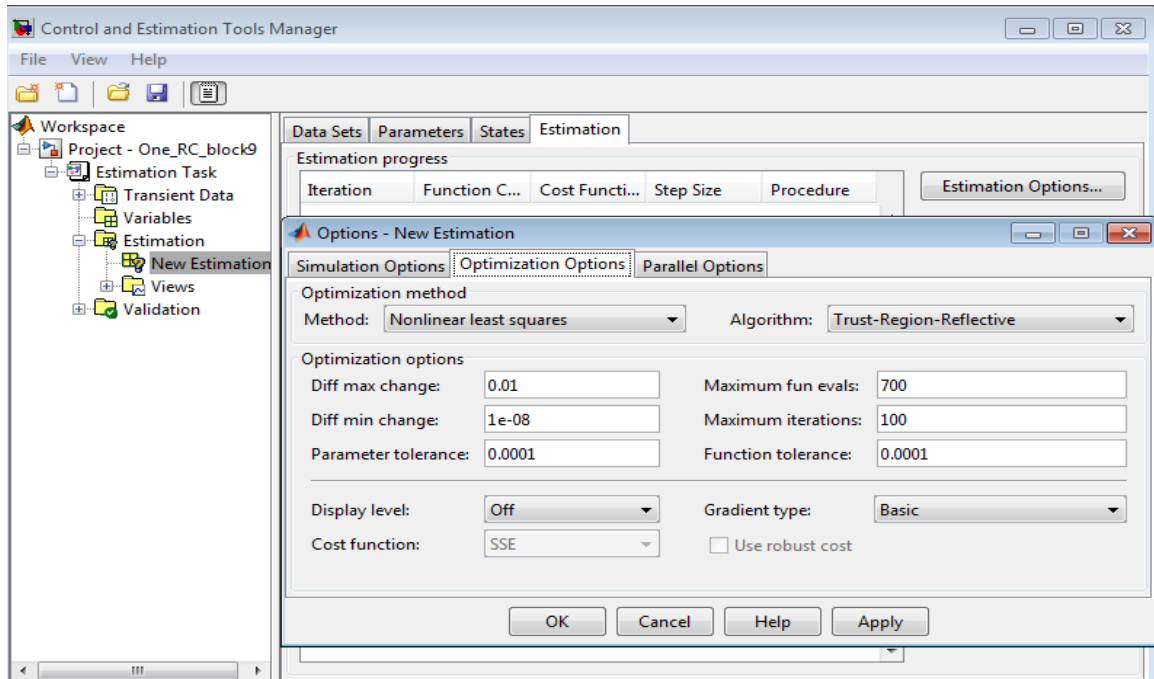


Figure 12: Estimation Routine in Simulink 2014a Parameter Estimation Toolbox

Acceptable results were obtained after proper dialogue box settings. Choosing logical bounds for the estimated parameters, as well as changing the parameter tolerance, the function tolerance and the maximum function evaluations were key to the system validation.

3.2.3 Vehicle Power System Model

The vehicle model can be described in three sections. The driver model consists of a ramp with a slope matching the experimental data. The ESS is described in detail in the previous section. The power system is a diesel series PHEV with a traction motor, ICE, generator and mobility model.

A 1.7 Liter diesel engine is connected to a three phase inverter and an interior permanent magnet motor delivering a continuous rated power of 42kW and a peak generating power of 71kW. The energy storage system (ESS) uses a 16 kW-hr Lithium-

Ion battery with a nominal bus voltage of 292V. The battery pack is connected to a 2.2kW DC-DC converter auxiliary power unit that provides 12V to the vehicle. The three phase inverter is connected to the electric motor and they both have a rated peak power of 145kW at a bus voltage of 320V. The electric motor is coupled with a single speed transmission with a final drive gear ratio of 9.59:1 providing power to the wheels.

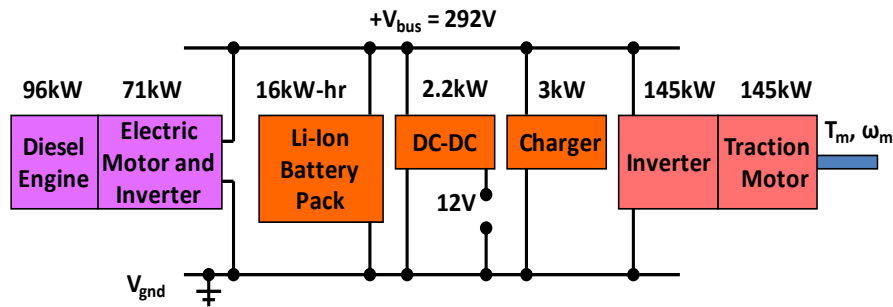
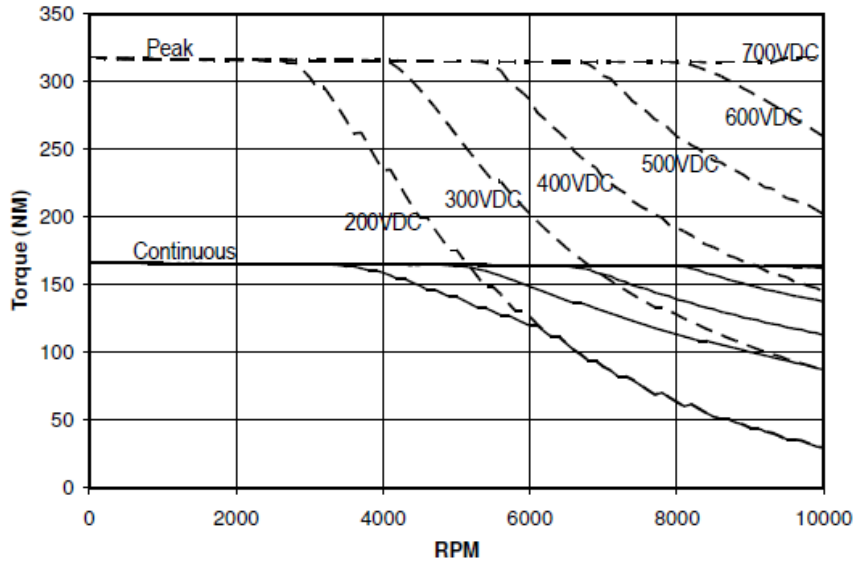


Figure 13: High Voltage Power System Components [22]

3.2.3.1 Traction Motor Model

The traction motor is modeled as a four quadrant electric machine. There are constant torque and constant power regions, below and above the break speed, respectively. Operating in forward motoring mode results in positive voltage and current and operating in regeneration mode results in positive voltage and negative current. The torque speed map was initially a static motor torque as a function of T_{max} and constant P_{max} . This provided good agreement with experimental data below the break speed w_b , but the simulated vehicle speed deviated significantly from experimental data above the break speed in the constant power region. Changing P_{max} allowed good agreement for the EV-only mode but not the hybrid performance mode, or vice-versa.

Allowing the P_{max} value to change as a function of bus voltage and current caused the modeled results to match for both EV-only and HEV performance mode.



**Figure 14: Remy HVH250-090P torque as a function of DC bus voltage
Remy International Inc. datasheet figure reproduced with
Permission [22]**

The model provides a variable torque output as a function of efficiency, bus voltage and maximum motor current. The inputs and outputs of the model are shown in Figure 15.

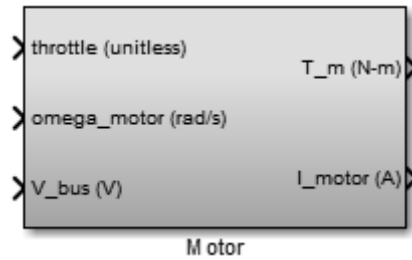


**Figure 15: Simulink motor model provides torque as a function of
throttle, speed and bus voltage**

$$T_m = \begin{cases} T_{max} \times throttle, & |w| < w_{max} \\ (P_{max}/|w|) \times throttle, & |w| \geq w_{max} \end{cases} \quad (18)$$

where w is the motor speed, T_{max} is the maximum motor torque and P_{max} is the maximum mechanical power found from,

$$P_{max} = V_{bus} \times i_{max} \times \eta_{motoring} \quad (19)$$

The motor model inputs are the motor speed and battery voltage and the outputs are motor torque and motor current. During motoring and generating, the current is found from equations (20) and (21) respectively,

$$i_{motor} = (1/\eta_{motoring}) \cdot (P_{mechanical} / V_{bus}) \quad (20)$$

$$i_{motor} = (1/\eta_{generating}) \cdot (P_{mechanical} / V_{bus}) \quad (21)$$

where P is the mechanical power $T_m * w_m$, V_{bus} is the bus voltage, and η is the efficiency which accounts for the energy loss during motoring or generating.

3.2.3.2 Engine / Generator

The simulated engine spins a generator to achieve a commanded power output and charge the battery with this power. The maximum engine torque $T_{e,max}$ is a mean value model from a torque speed map. The inputs and outputs of the ICE are shown in Figure 16.

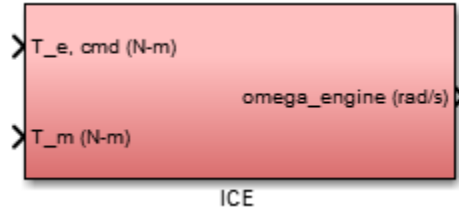


Figure 16: Engine Simulink model showing engine speed as a function of commanded torque and the motor's reaction torque

$$T_e = T_{e,actual} - T_{resistance} - T_m \quad (22)$$

where,

$$T_{e,actual} = T_{e,max} * u_{throttle} \quad (23)$$

Engine speed w_e is the integral of the sum of torques from commanded torque $T_{e,cmd}$, reaction torque T_m , and a Coulombic resistive torque $T_{resistive}$.

The generator is modeled in the same way as the motor in 3.2.3.1.

3.2.3.3 Mobility Model

The mobility model determines the vehicle's velocity as a function of tractive effort, rolling resistance, aerodynamic drag and slope [25]. The vehicle acceleration is computed from,

$$a_x = \frac{\sum F}{(m + m_r)} = \frac{F_x - F_{rr} - F_{aero} - F_{slope}}{(m + m_r)} \quad (24)$$

where F_x is the tractive force, F_{rr} is the tire rolling resistance force, F_{aero} is the aerodynamic drag, F_{slope} is the grade force caused by a vehicle going uphill or downhill,

m is the vehicle mass and m_r is the equivalent rotational mass. The vehicle velocity is found by integrating the acceleration (24).

3.3 Experimental Apparatus

3.3.1 Battery Test Procedure

Two discharge tests were conducted at Embry-Riddle Aeronautical University's chassis dynamometer. ESS data was collected during vehicle chassis dynamometer operation in electric-only, or charge depleting mode. First, the battery of a modified 2013 Chevrolet Malibu hybrid vehicle was fully charged and the battery cells were balanced prior to vehicle operation. Cell balancing ensures that all cells in the battery pack have an identical voltage. The battery management system uses resistors to bleed power out of higher voltage cells to achieve voltage uniformity across the pack. The battery's SOC was at 99% before the start of each test.

To ensure complete voltage stabilization, the vehicle was at rest for a period of 24 hours. The vehicle's wheels were placed on the Dynamometer drum and the parking brake was turned on. The vehicle was tightly tied down using the Dynamometer straps and the Dynamometer strap points on the ground. The lab's garage door was open and the cooling fan was turned on and placed in front of the vehicle with the air blowing on the front grill, as shown in Figure 17. In the Dynamometer controller, the electric motor's angular velocity was set to a constant 5000rpm with the torque changing with the applied throttle.

In the first discharge test, the battery was discharged at a constant current of 100Amps by applying a constant throttle in coordination with the dynamometer's resistive load. The Vector Data Logger recorded all the experiment outputs including battery current

voltage, state of charge and temperature. The Battery's SOC was at 94% at the start of the test and was discharged down to 30% instead of 0% to avoid battery deterioration.

In the second discharge test, the battery was discharged in an extended test with eight sequential discharge rates: 20Amps, 40Amps, 60Amps, 80Amps, 100Amps, 120Amps, 140Amps and 50Amps. Finally, the Vector Data Logger recorded all the outputs.

The battery's temperature was set to hold a constant temperature of 31°C, when the temperature goes over this value, the coolant kicks in. Typically, the cells on the outer part of the pack have a lower temperature while the cells in the middle part have a hotter more uniform temperature of 31°C.

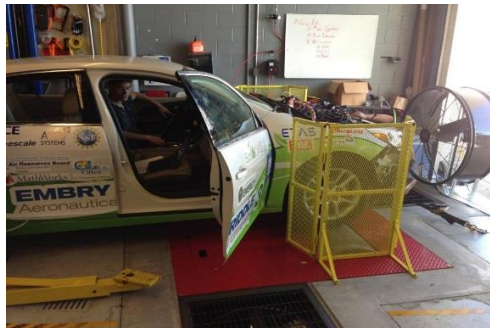


Figure 17: Vehicle on dynamometer drum

3.3.2 Maximum Acceleration 0-60mph Vehicle Tests

A modified 2013 Chevrolet Malibu hybrid electric vehicle was subject to two maximum acceleration tests from 0-60mph. Both tests were performed on the same stretch of dry, flat pavement with the same driver and passenger on board and in the same direction of travel to ensure uniformity. Test #1 was a maximum acceleration test from 0-60mph in

EV-only mode, where the ESS was the sole power source. The driver applied full throttle until the vehicle speed slightly exceeded 60mph. Test #2 was a maximum acceleration from 0-60mph in HEV mode or launch control mode. The driver pressed a dashboard button, shifted into neutral, applied full throttle, and then switched the shift lever from Neutral to Drive. In Test #2 the engine generator operated in charge sustaining mode providing power to the ESS through the high voltage bus. Shifting from Neutral to Drive allowed the SCU to command maximum torque to the traction motor and inverter. Detailed test results are presented in [22].

Chapter IV

Results

This chapter presents the results of the validated battery model and the validated vehicle launch control model. The values of the estimated parameters are shown and the simulated output is compared against the measured data.

4.1 Battery Model

Two discharge tests were conducted and simulated in order to compare the measured and simulated data. Simulink Parameter Estimation Toolbox was used to identify the uncertain parameters R_{00} and A_0 in (13), R_{10} in (11) and the open circuit voltage OCV which is a lookup table in Simulink varying with the state of charge. The parameter trajectories are shown in Figure 18 and the parameter values are shown in Table 2. Figure 16, shows that the optimized parameters converged after 7 iterations, which means that the specified parameter or function tolerance was reached. The OCV has a different value at every state of charge breakpoint, which explains the multiple signal trajectories in Figure 18.

The parameter estimation toolbox successfully output a monotonically increasing OCV which was not monotonically increasing initially. Notice R_{10} changed sign because of uncertainty in the initial guess. Both of these changes are realistic according to the physical system.

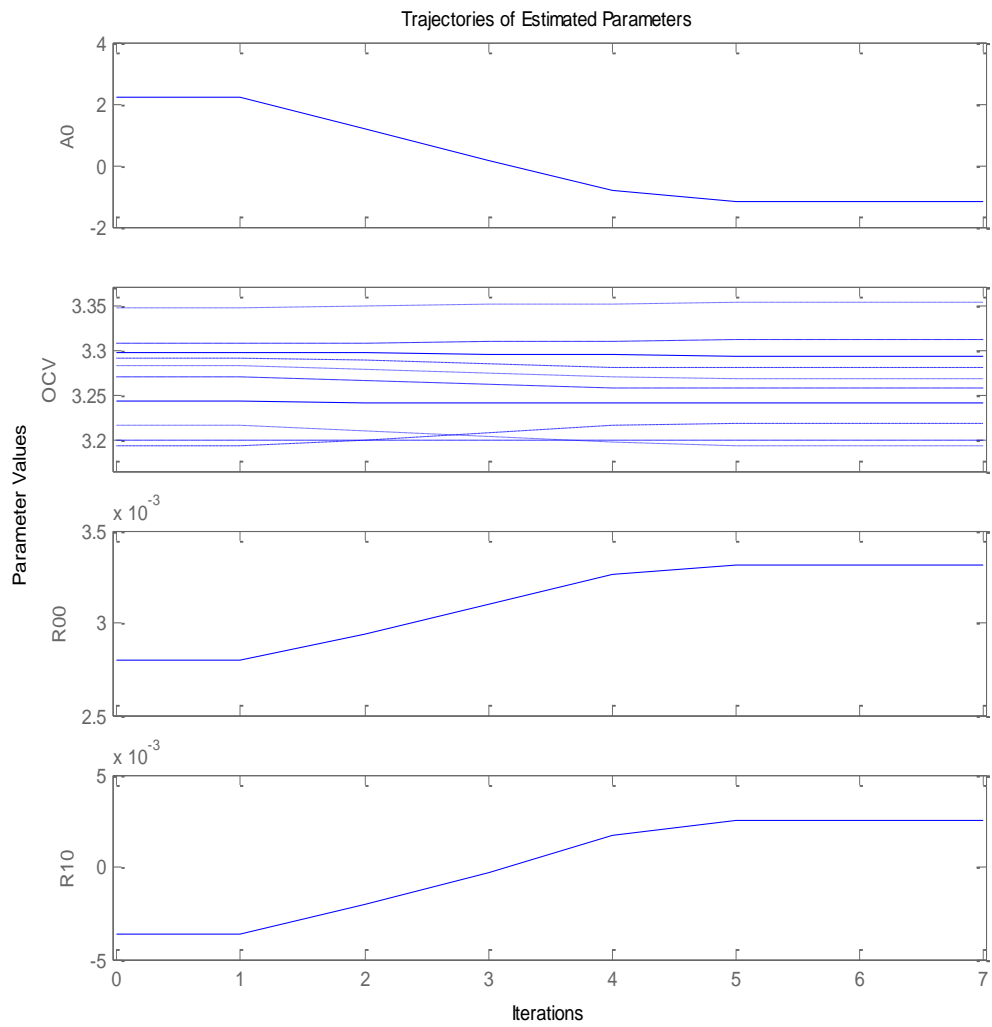


Figure 18. Parameter trajectories showing convergence

Table 2: Estimated battery parameters using Simulink Design Optimization Toolbox 2014a

A_0 (unit less)	-1.1976	
R_{00} (Ohms)	0.0033	
R_{10} (Ohms)	0.0025	
OCV = fcn(SOC)	OCV (V)	SOC (%)
	2.25	0
	3.2	10
	3.1934	20
	3.2196	30
	3.2416	40
	3.2571	50
	3.2688	60
	3.2803	70
	3.2941	80
	3.3109	90
3.3526	100	

4.1.1. Discharge Test 1

The experimental discharge current of 100 Amps was input to the battery model. Figure 19 shows the simulated and measured terminal voltage along with the applied discharge current. The mean squared error between measured and simulated data is 0.26 volts.

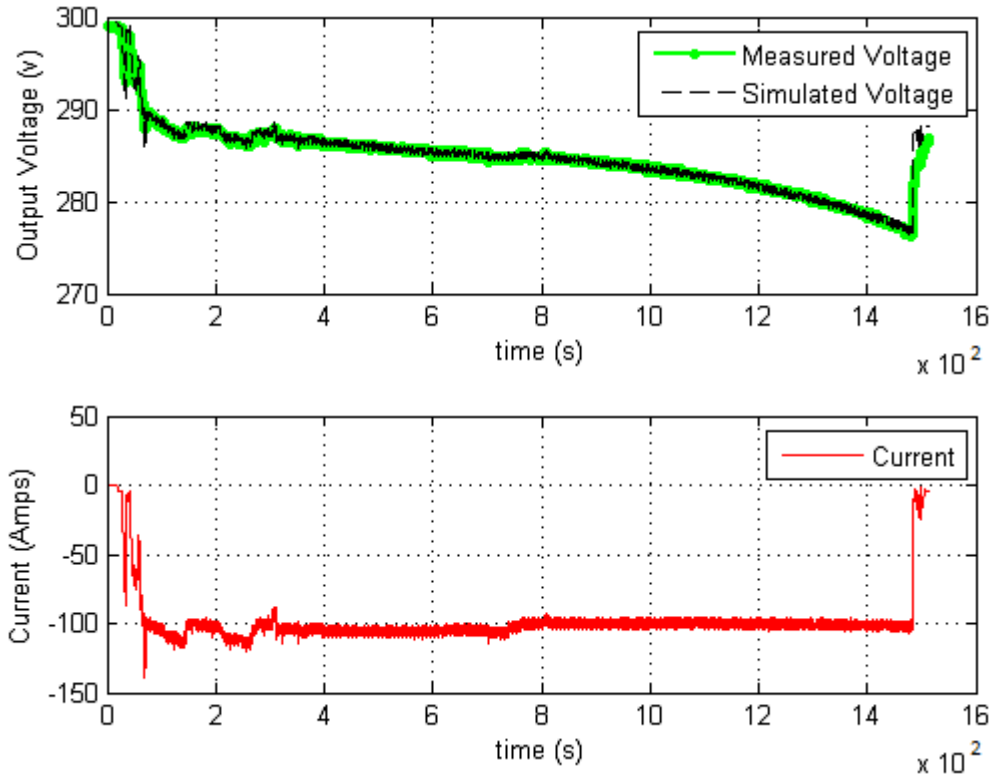


Figure 19: Measured and simulated voltage for a discharge current of 100 Amps

Figure 20 shows the simulated and measured SOC at a discharge current of 100 Amps. The mean squared error between measured and simulated data is $6.07e^{-4}$ (%).

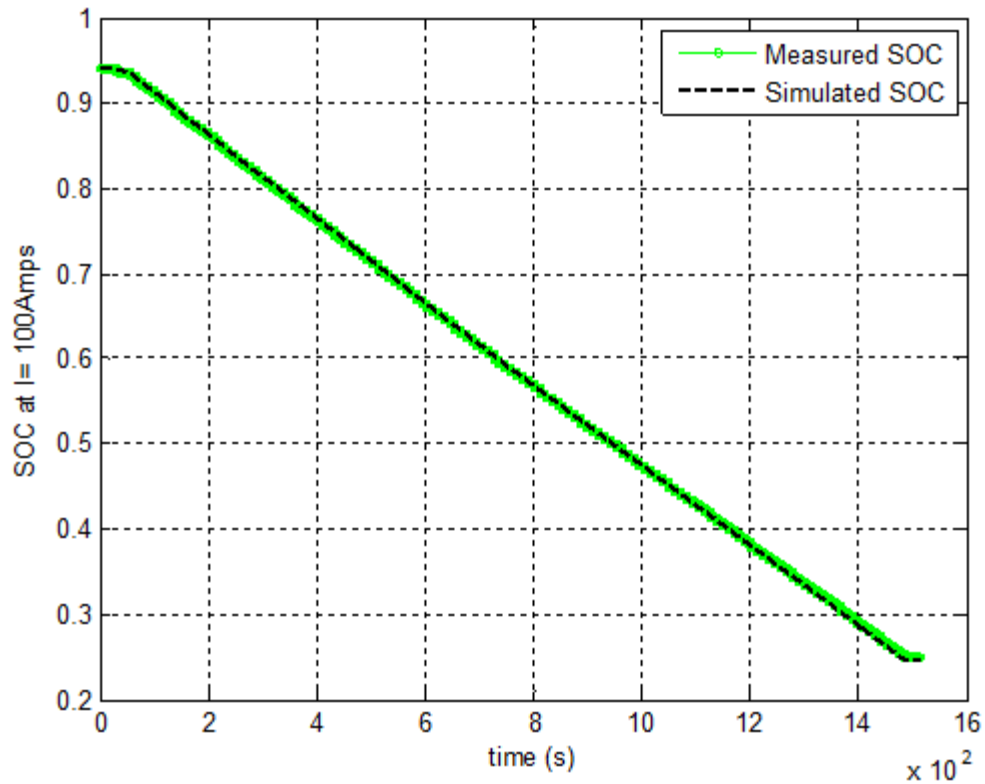


Figure 20: Measured and simulated SOC for a discharge current of 100 Amps

4.1.2. Discharge Test 2

A variable discharge current was input to the battery model for discharge test 2. Figure 21 shows the simulated and measured terminal voltage along with the variable discharge current applied. The voltage changes at every discharge rate: the higher is the discharge current applied, the lower is the voltage. The mean squared error between measured and simulated data is 0.21 volts.

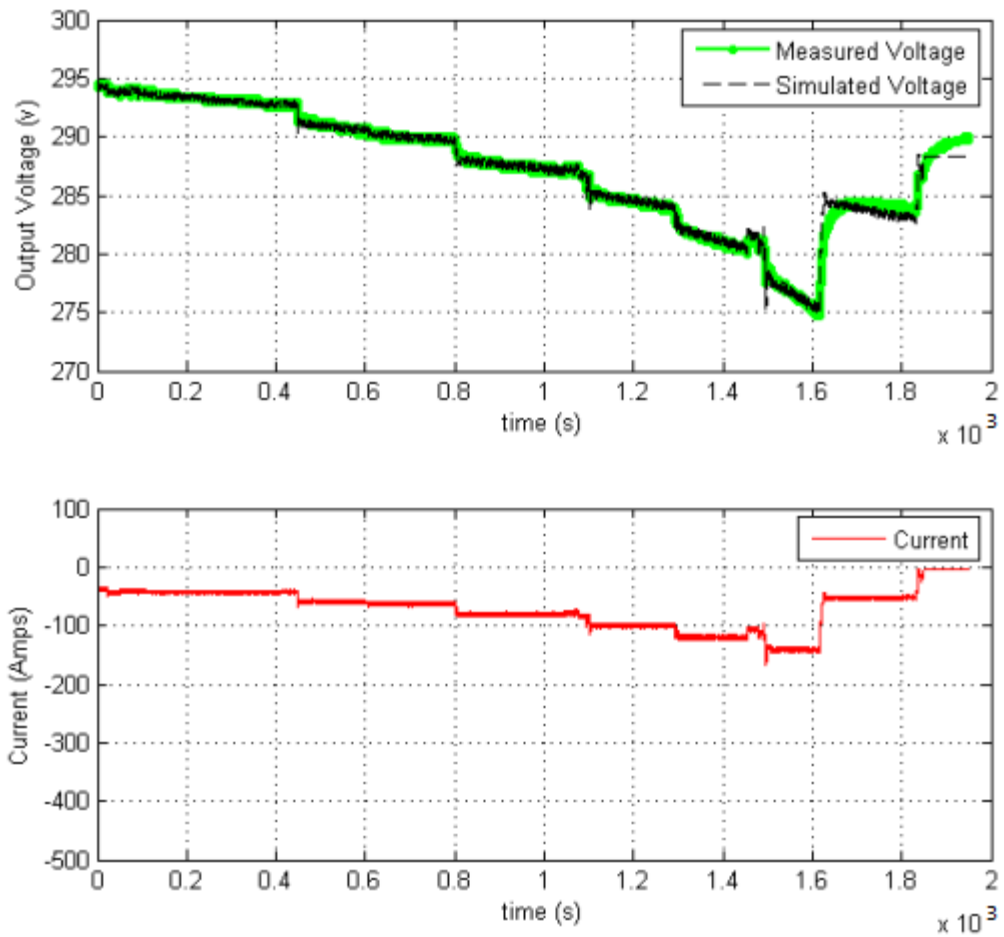


Figure 21: Measured and simulated voltage for a variable discharge current

Figure 22 shows the simulated and measured SOC. The mean squared error between measured and simulated data is $9.25e^{-4}$ (%). Notice a dip in SOC below 30%, this is due to the discharge current change from 140 Amps to 50 Amps then to 0 Amps.

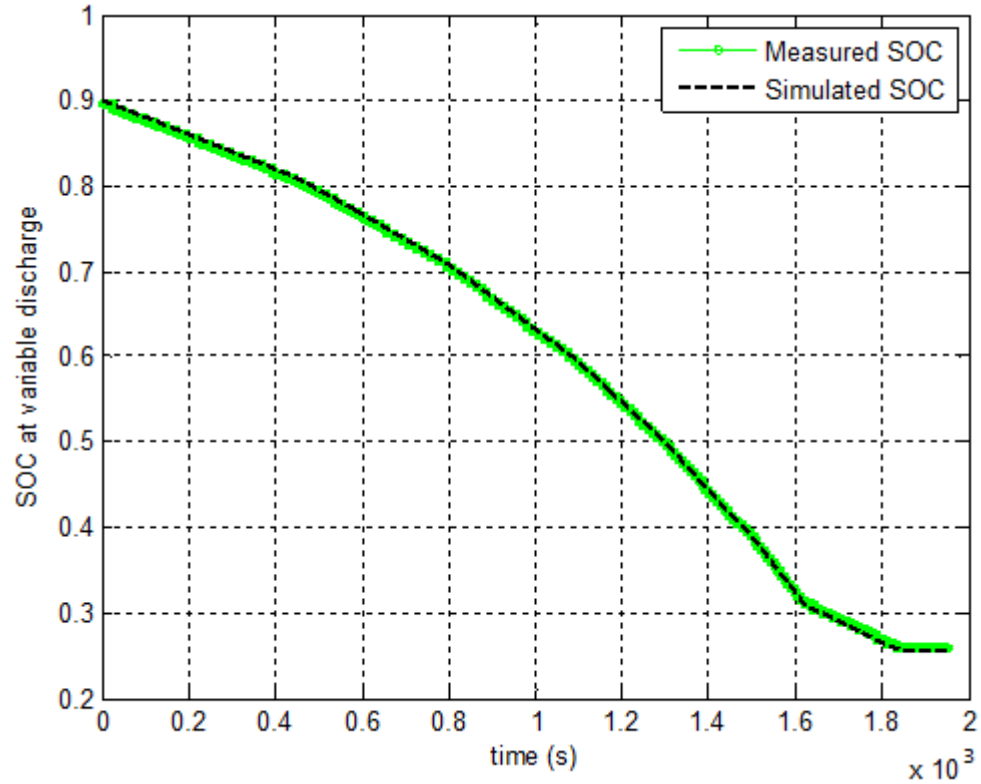


Figure 22: Measured and simulated SOC for a variable discharge current

4.2 Vehicle Model 0-60mph Acceleration Tests

A hybrid electric vehicle was subject to two maximum acceleration tests. Test 1 represents a 0-60mph acceleration in EV-mode and test 2 represents a 0-60mph in HEV mode. Simulink Parameter Estimation toolbox was used to identify uncertain parameters in order to validate the simulated vehicle speed with test data. These parameters are the tire rolling resistance coefficient μ_{rr} , the maximum current i_{max} and the maximum torque T_{max} . The values of the maximum current and torque are usually available in manufacturer datasheet but these are only estimates pertaining to specific conditions. For example the maximum torque and power for the Remy HVH250-090P motor were 318Nm and 145kW peak, respectively, for a bus voltage of 320V while testing used a

292V bus voltage. Derating or scaling manufacturer datasheet was necessary to portray the test conditions. The estimated parameters values are shown in Table 3.

Table 3. Estimated Vehicle parameters using Simulink 2014a Optimization toolbox

Estimated Parameters	Values
μ_{rr} (unit less)	.015
i_{max} (Amps)	512
T_{max} (Nm)	290

4.2.1. Vehicle Test 1 and Test 2

All vehicle data was collected via 100Hz CANbus messages from on-board vehicle sensors and subsystem components. The starting time for both tests was selected in the data logs as the first non-zero torque value reported by the traction motor inverter. The stopping time was selected as the first logged speed value to exceed the 60mph threshold. A torque-based starting time and speed based stopping criteria ensures uniformity in comparing 0-60mph times by eliminating driver response time [22].

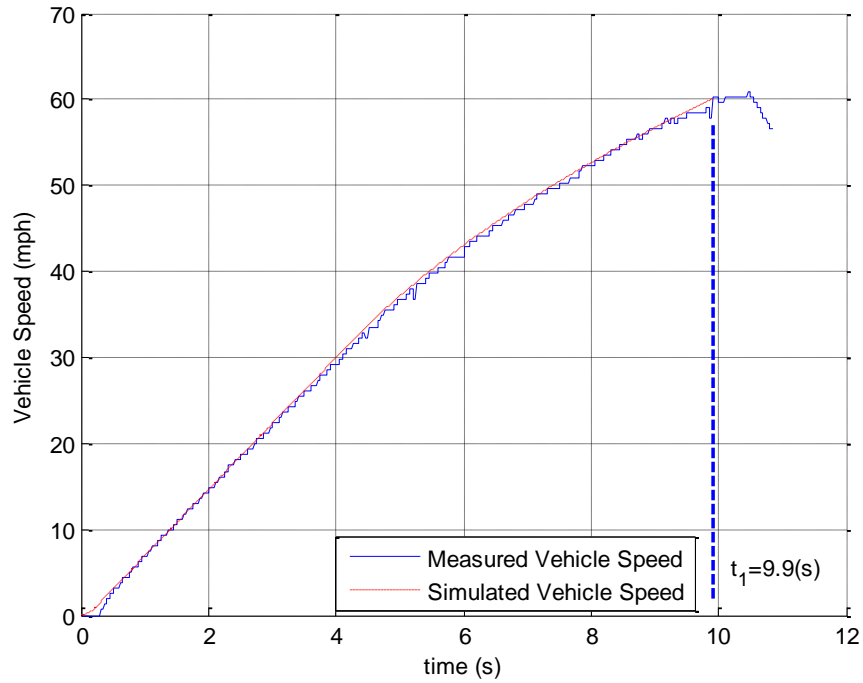


Figure 23: Maximum Acceleration from 0-60mph validation in EV-mode

In test 1, the vehicle was simulated under maximum acceleration from 0-60mph in EV-mode. The ESS was the only source of power and mobility. Figure 23 shows measured vehicle speed against simulated speed. The maximum speed of 60 mph is reached at $t=9.9$ sec. The measured vehicle speed is a straightforward measurement therefore has a high accuracy level. The vehicle speed during [0 4] sec characterize the torque limited region and the simulated curve was highly influenced by the maximum torque value. The remaining time history represents the power limited region. Bus voltage was measured during the test so the parameter varied was an assumed constant maximum current i_{max} , as in (19). The simulated curve was highly influenced by the

maximum current value. A variable break speed motor was necessary to match the data due to the variation in bus voltage.

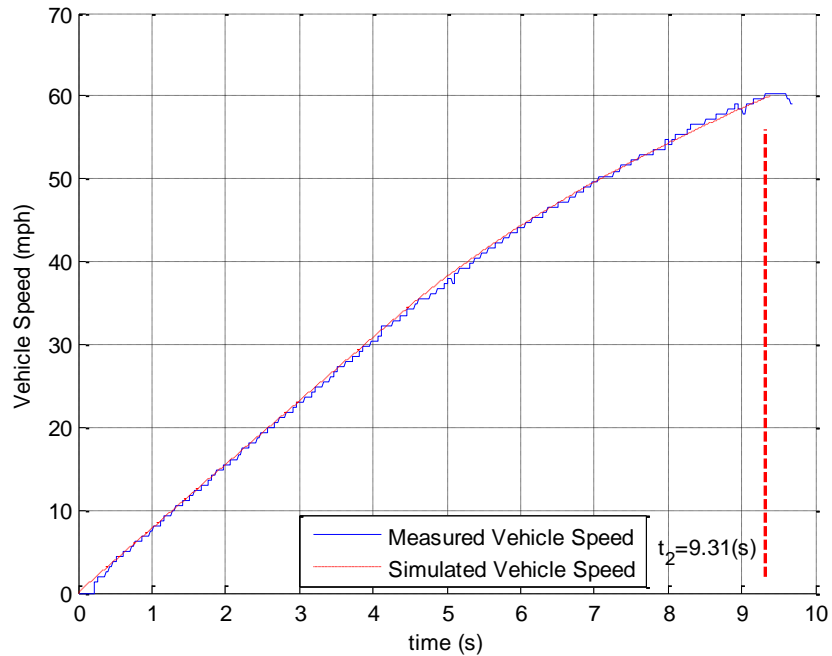


Figure 24: Maximum Acceleration from 0-60mph validation in HEV-mode

In test 2, the vehicle was simulated under maximum acceleration from 0-60mph in HEV-mode. The engine generator was placed in charge sustaining mode which provided additional power to the traction motor. Figure 24 shows measured vehicle speed against simulated speed. The maximum speed of 60 mph is reached at $t=9.31$ sec. The torque limited region is represented from [0 4]sec, the maximum torque value highly influenced the validation of the simulated speed in this region. The remaining time history represents the power limited region where the maximum current influenced the speed validation. Notice in Figures 21 and 22, a time delay prior to $t=0.30$ s between

measured and simulated vehicle speed. This is due to driveline compliance in rotating components between the traction motor and the tires.

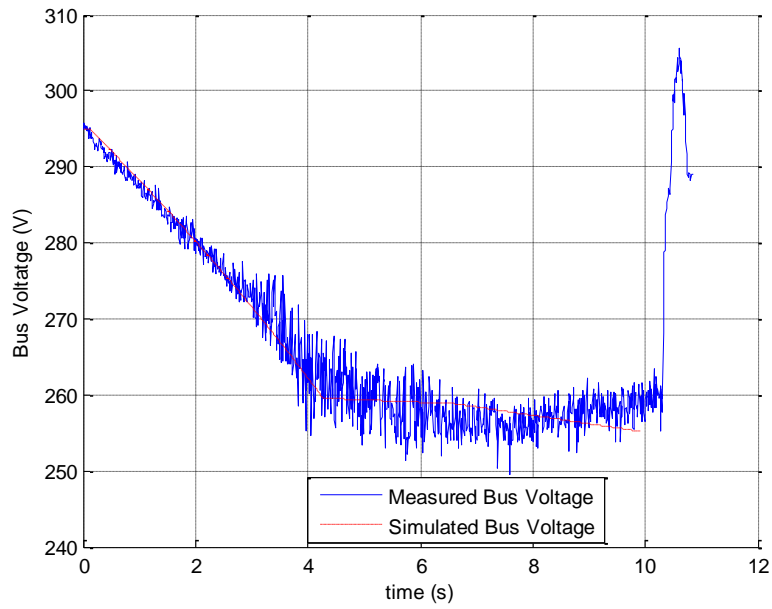


Figure 25: Bus Voltage validation in EV- mode

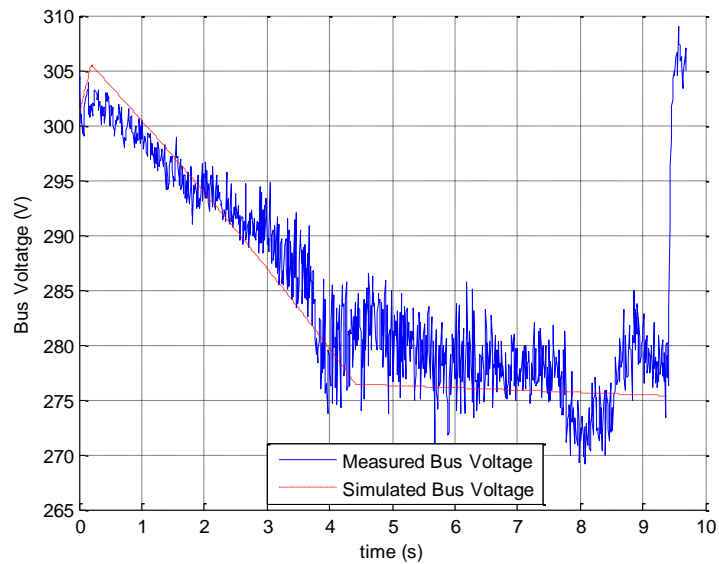


Figure 26: Bus Voltage validation in HEV- mode

Figure 25 and Figure 26 show the bus voltage validation in EV and HEV modes respectively. In the power-limited region, the mean bus voltage is 258 volts in EV-mode and 277 volts in HEV mode. The increase in bus voltage is due to the power system being in charge sustaining mode prior to the vehicle launch. The bus voltage sensors provide high accuracy measurements.

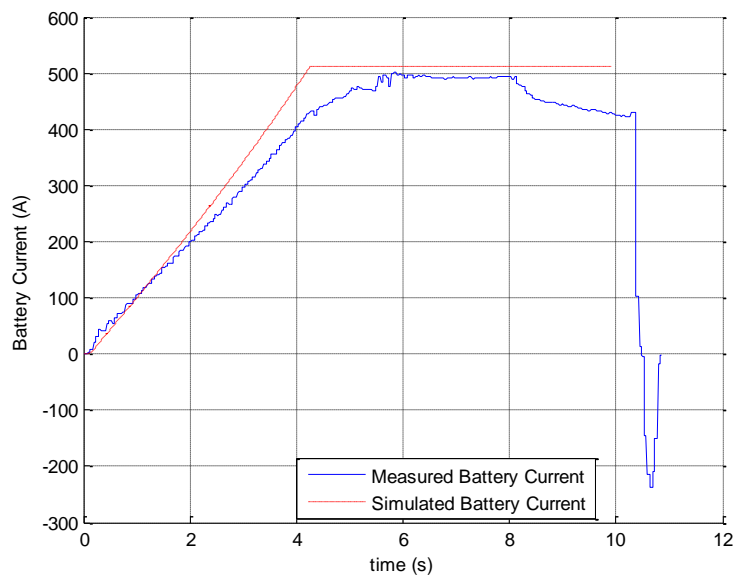


Figure 27: Measured and simulated battery current in EV-mode

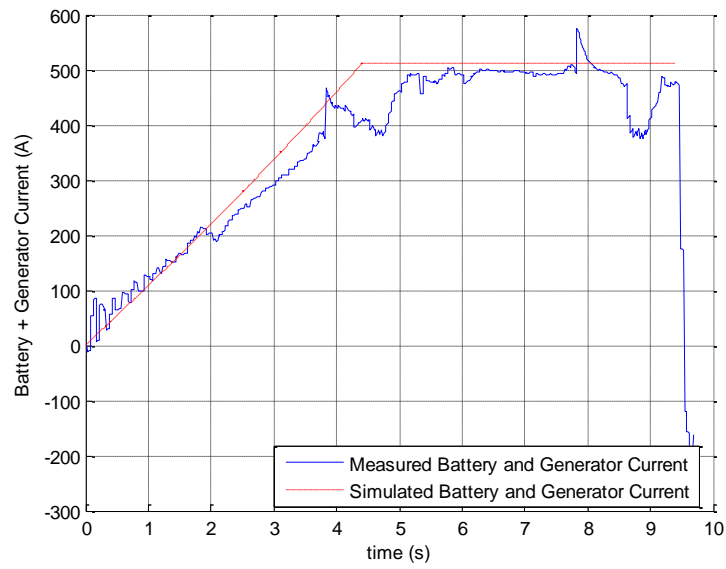


Figure 28: Measured and simulated battery and Generator current in HEV-mode

Figure 27 shows the battery current validation in EV-mode. The maximum simulated battery current is 512 Amps, and the maximum measured current is 500 Amps. Figure 28 shows the battery and generator current validation in HEV mode. These figures show that both tests were performed with the same current draw. The current estimate is low fidelity because it does not account for inverter losses, so the actual current would be slightly higher.

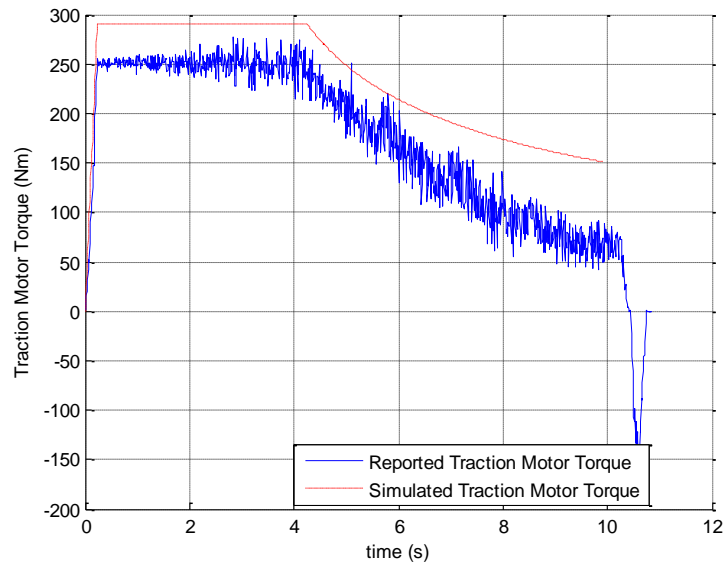


Figure 29: Measured and simulated traction motor torque in EV-mode

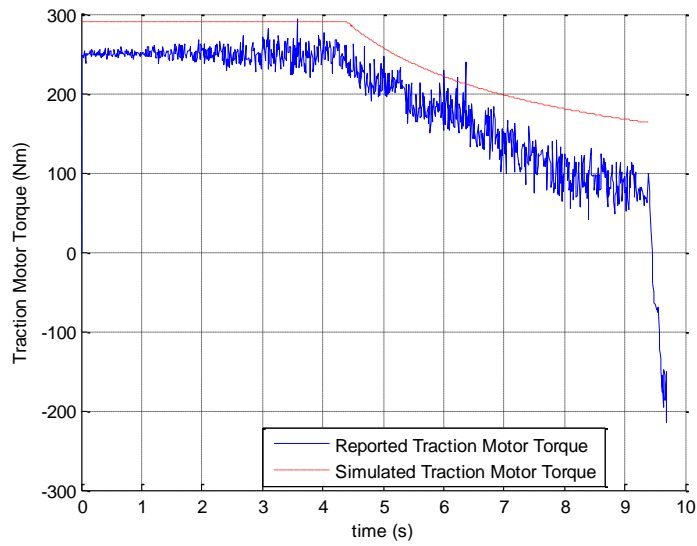


Figure 30: Measured and simulated traction motor torque in HEV-mode

Figures 29 and Figure 30 show the reported traction motor torque validation in EV and HEV mode respectively. Both torque figures show a constant torque region followed

by a power-limited region. The reported and simulated torques have the same break speed slightly after $t=4\text{sec}$. There is a 16% error between simulated and reported torque. The reported motor torque is a low accuracy measurement. The torque estimate relies on sensor measurements combined with offline finite element analysis under static conditions. Other causes of torque low fidelity are motor-to-motor variations and temperature variations. Further detailed discussion is presented in [22].

Chapter V

Discussion, Conclusions, and Recommendations

This chapter presents discussions and conclusions on Parameter Optimization for the ESS and vehicle model and recommendations for future work.

5.1. Parameter Optimization Theory

Parameter optimization is a powerful and effective method for validating physical system models with experimental test data. The formal optimization problem statement as presented in this thesis has not been found in a textbook. Similar problem statements are available for optimal control but not for model validation. Simulink Design Optimization toolbox was a convenient tool for model validation.

5.2 ESS Parameter Optimization

A battery model has been created and validated for the EcoCAR2 Chevrolet Malibu. Parameter estimation was conducted using Simulink to determine the constants in (11) and (13). The simulated voltage and state of charge match the experimental outputs. For the constant current discharge, the mean square error between measured and simulated data was 0.26 volts for the terminal voltage, and $6.07e^{-4}$ (%) for the state of charge. For the extended variable current discharge, the mean square error between measured and simulated data was 0.21 volts for the voltage and $9.25e^{-4}$ for the state of charge. The battery model was implemented in a hybrid electric vehicle model.

5.3 Vehicle Parameter Optimization

Parameter estimation was conducted to validate a launch control strategy presented in [22]. The vehicle was modeled for two maximum acceleration tests from 0-60mph. Test 1 represents the maximum acceleration in EV-only mode, where the ESS

was the sole source of power, and test 2 represents the maximum acceleration in HEV mode or launch control mode. The 0-60mph time was found to be 9.9sec in test 1 and 9.31sec in test 2, which validates the experimental results. In test 1, the root mean square error between measured and simulated data is 0.52 mph for vehicle speed and 2.68V for voltage. In test 2, the root mean square error between measured and simulated data is 0.43 mph for vehicle speed and 3.50V for voltage. The estimated parameters were maximum torque, maximum current and tire rolling resistance.

Parameter estimation was necessary in order to match and validate the model with the measured data. Parameters representing the electric drive components are provided in manufacturer datasheets that did not match the experiment operating conditions. The parameter optimization toolbox helped estimate these unknown parameters better to allow the models to match experimental data. The motor speed and bus voltage measurements were assumed of high accuracy, while motor torque and current have a lower accuracy level because they are estimated from sensor measurements and offline finite element analysis which is subject to modelling error along with temperature and manufacturing variations. The parameter optimization toolbox provided a convenient framework to prioritize different sensor measurements based on these confidence levels.

5.2. Recommendations

The parameter optimization routine searches for an optimal solution to match modeled and measured data with respect to chosen parameter and function tolerances. Changing the tolerances would allow the optimization to find more accurate results. The battery model does not account for changes in performance due to temperature variations, therefore developing a thermal model could be of high advantage. Finally,

manufacturer's data is rated under specific conditions that do not match the test conditions. Using these specific values in vehicle performance simulations would not lead to accurate simulation results. Therefore, developing a derating or scaling strategy to match the test conditions would be highly beneficial.

Appendix A

Bibliography

References

- [1] Smith, B.,S., Raj,L.,S.,A., Wong, G., 2012, "Intelligent Control System for Improving the Efficiency of a Series Hybrid for the EcoCAR 2 Challenge," IEEE Southeastcon Proceedings, pp. 1-5.

- [2] Ehsani, M., Gao,Y.,Emadi,A., 2009, "Modern Electric, Hybrid Electric, and Fuel Cell Vehicles,"CRC Press.

- [3] Momoh,O.D.,Omoigui,M.O., 2009, "An Overview of Hybrid Electric Vehicle Technology," IEEE Vehicle Power and Propulsion Conference, pp. 1286-1292.

- [4] Simpson, A., 2006, "Cost-Benefit Analysis of Plug-in Hybrid Electric Vehicle Technology," National Renewable Energy Laboratory.

- [5] Junnuri, R. K., Shivaram, K., Annamalai, R., 2014, "Optimization Based System Identification of HEV Li-Ion Battery," Controls, Measurement and Calibration Congress.

- [6] Borghesani, C., and Eryilmaz, B., 2014, "Improve the Fidelity of Your Simulink Models using Test Data and Parameter Estimation," Mathworks.

- [7] Mathworks, 2014, "Estimate Parameters from Measured Data," 2015.

- [8] Mathworks, 2014, "Simulink Design Optimization," 2015.

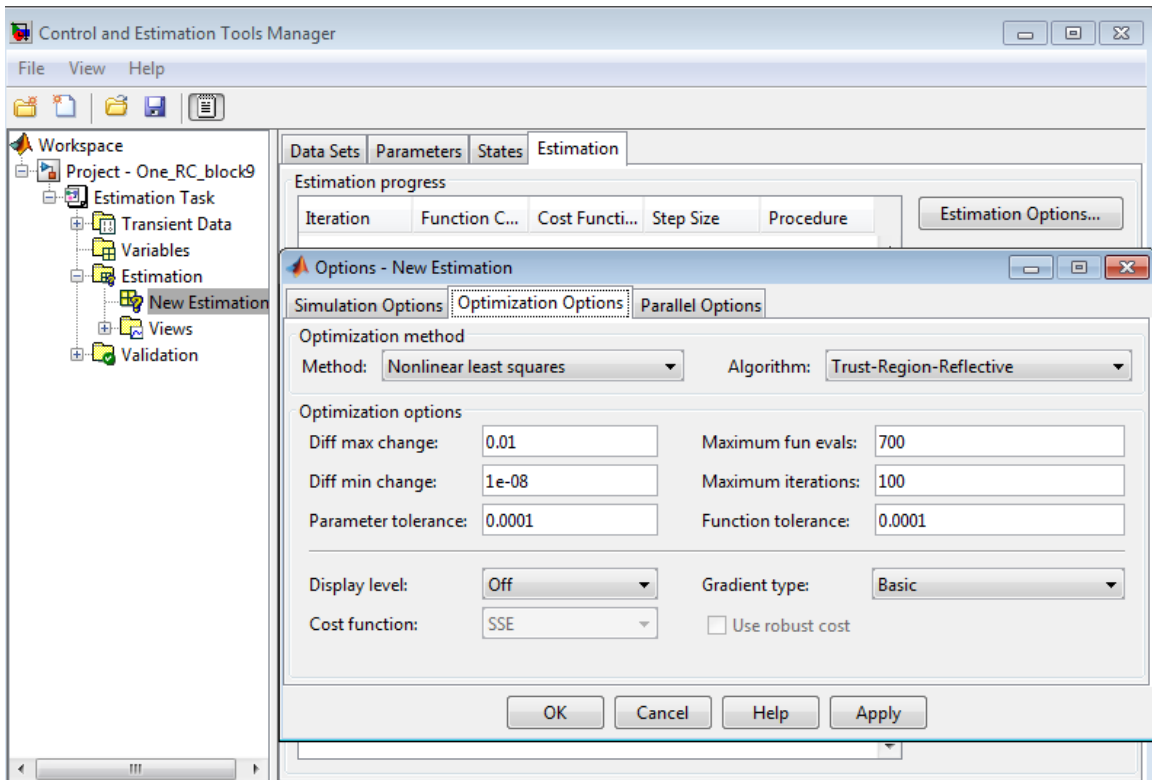
- [9] Mathworks, 2014, "Optimization Options," The MathWorks, Inc., 2015(3/5) .

- [10] Hieb, B., 2013, "Creating a High-Fidelity Model of an Electric Motor for Control System Design and Verification," The MathWorks, Inc..
- [11] Hull, D. G., 1996, "Conversion of Optimal Control Problems into Parameter Optimization Problems," AIAA Journal of Guidance, Control and Dynamics, **20**.
- [12] Jager, B.d., Keulen, T.V., and Kessels, J., 2013, "Optimal Control of Hybrid Vehicles," Springer, London, pp. 39.
- [13] Slotine, J.J.E., and Li, W., 1991, "Applied Nonlinear Control," Prentice Hall, Inc., New Jersey, pp. 311.
- [14] Shafiei, A., Momeni, A., Williamson, S., 2011, "Battery Modeling Approaches and Management Techniques for Plug-in Hybrid Electric Vehicles," IEEE Conference Vehicle Power and Propulsion Conference, pp. 1-5.
- [15] Chan, H.L., Sutanto, D., 2000, "A New Battery Model for use with Battery Energy Storage Systems and Electric Vehicles Power Systems," IEEE Power Engineering Society Meeting, pp. 470-475.
- [16] He, H., Xiong, R., Fan, J., 2011, "Evaluation of Lithium-Ion Battery Equivalent Circuit Models for State of Charge Estimation by an Experimental Approach," Energies, (Electric and Hybrid Vehicles).
- [17] Kroeze, R.C., Krein, P.T., 2008, "Electrical Battery Model for use in Dynamic Electric Vehicle Simulations," IEEE Power Electronics Specialists Conference, pp. 1336-1342.

- [18] Barsali,S., Ceraolo,M., 2002, "Dynamical Models of Lead-Acid Batteries: Implementation Issues," IEEE Transactions on Energy Conversion, pp. 16-23.
- [19] Jackey, R. A., 2007, "A Simple, Effective Lead-Acid Battery Modeling Process for Electrical System Component Selection," The MathWorks, Inc..
- [20] Huria,T.,Ceraolo,M.,Gazzarri,J.,Jackey,R., 2012, "High Fidelity Electrical Model with Thermal Dependence for Characterization and Simulation of High Power Lithium Battery Cells," IEEE Electric Vehicle Conference, pp. 1-8.
- [21] Jackey,R.,Saginaw,M.,Sanghvi,P.,Gazzarri,J.,Huria,T.,Ceraolo,M., 2013, "Battery Model Parameter Estimation using a Layered Technique: An Example using a Lithium Iron Phosphate Cell," The MathWorks, Inc..
- [22] Compere, M., Bonderczuk,D.,Khalifi,H.,Currier,P., Submitted 2015, "Electric Launch Control for a Series Hybrid Electric Vehicle," SAE.
- [23] Mathworks, 2014, "Least Square (Model Fitting) Algorithms," The MathWorks, Inc., **2015**(3/5).
- [24] Mathworks, 2014, "Choosing a Solver," The MathWorks, Inc., 2015(3/5).
- [25] Gillepsie, T.D., "Fundamentals of Vehicle Dynamics", Society of Automotive Engineers, 1992.

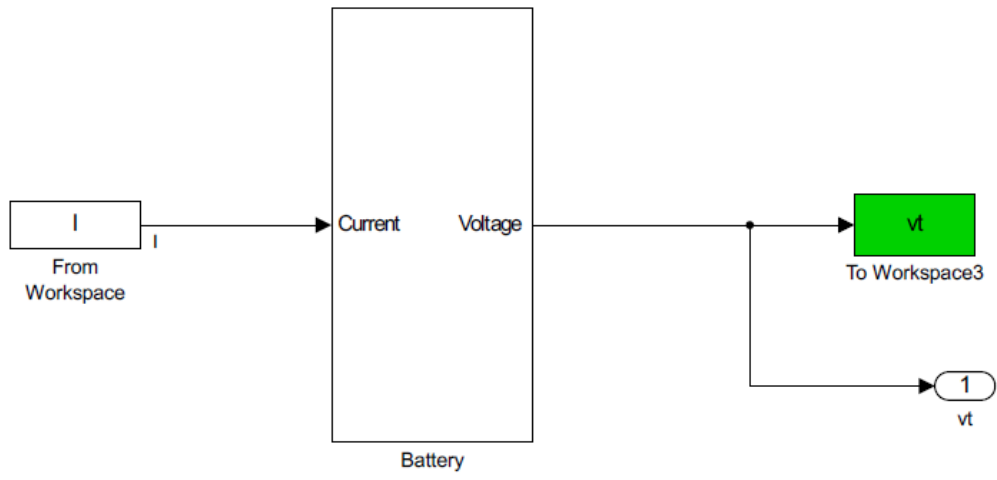
Appendix B

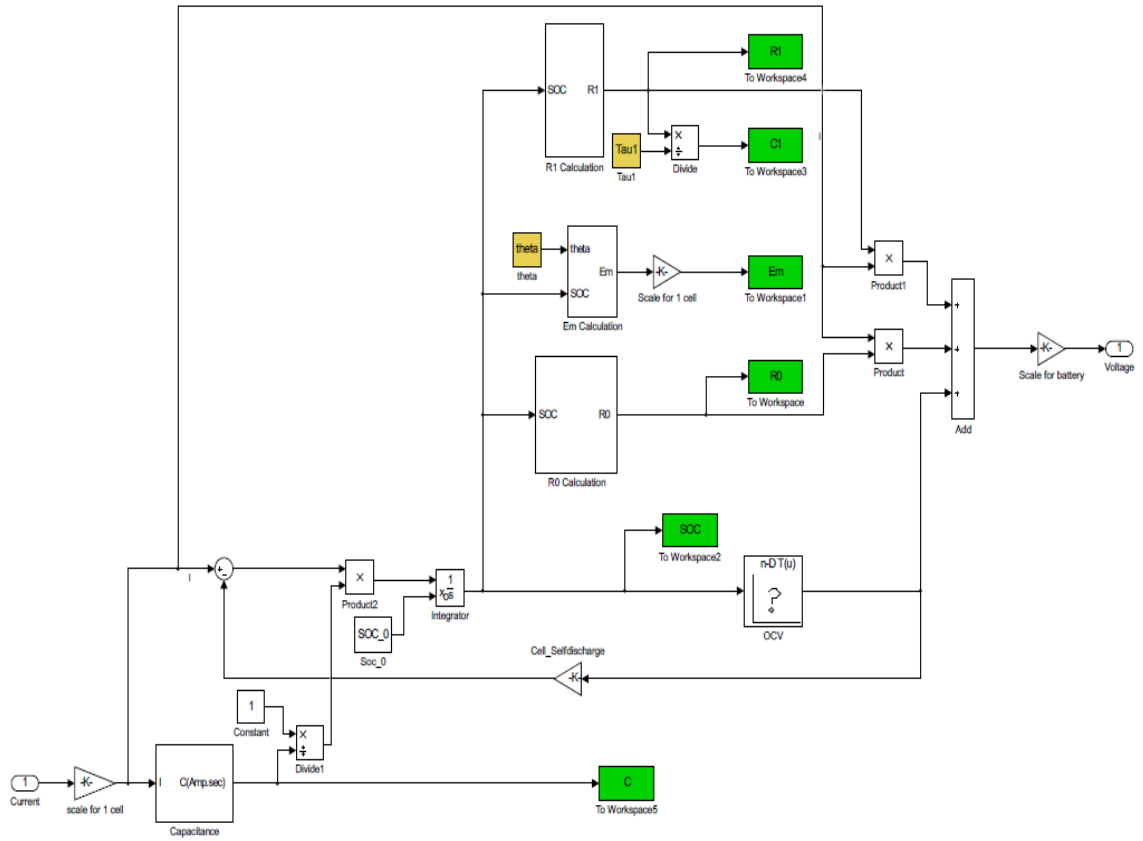
Simulink Optimization Toolbox

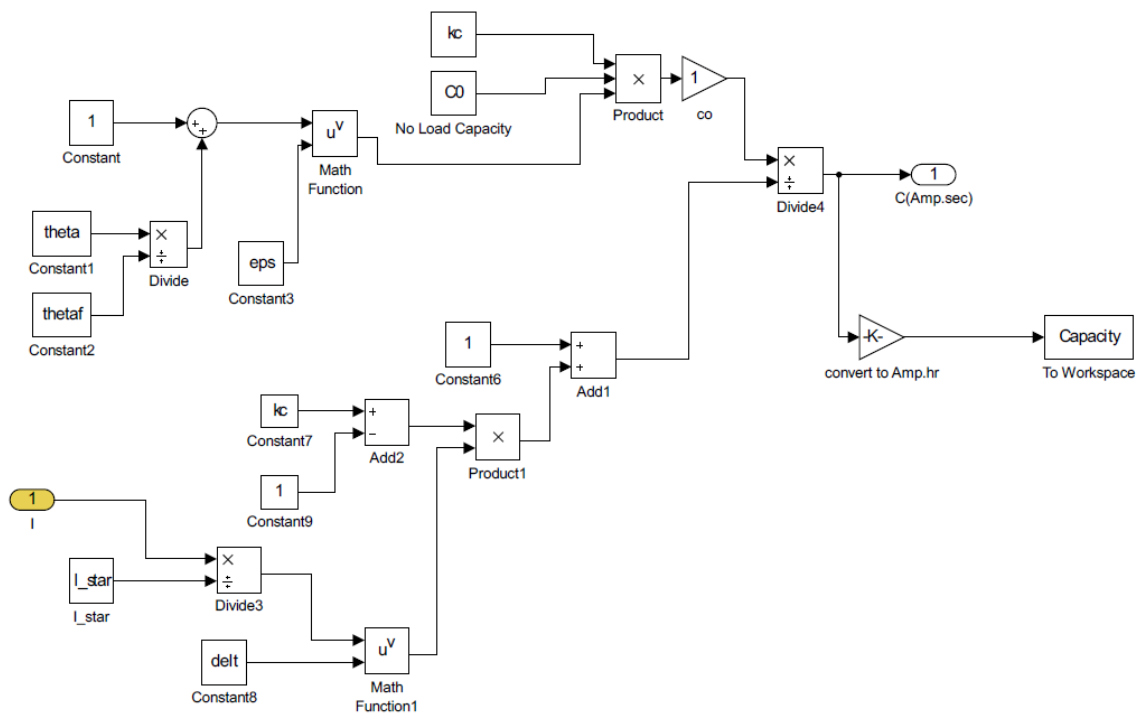


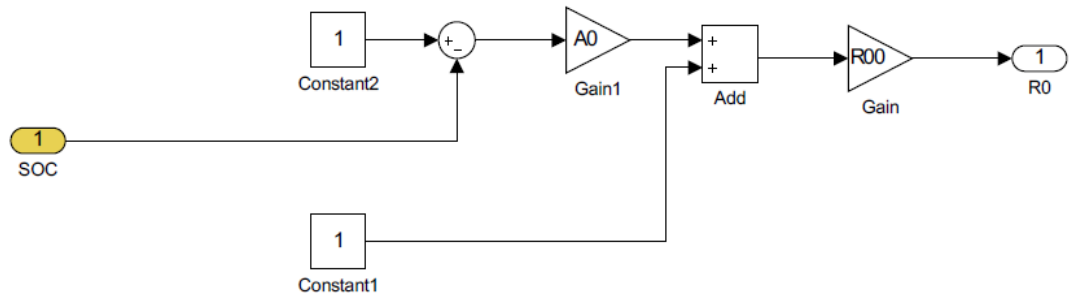
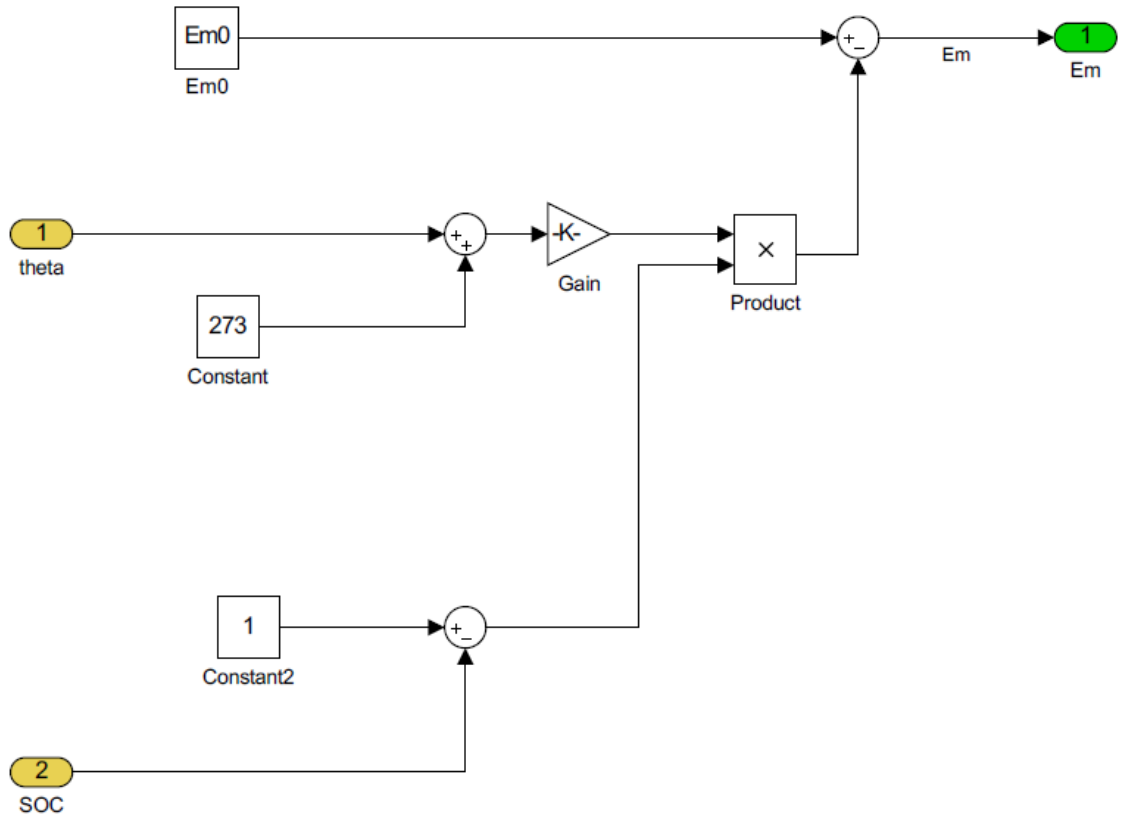
Appendix C

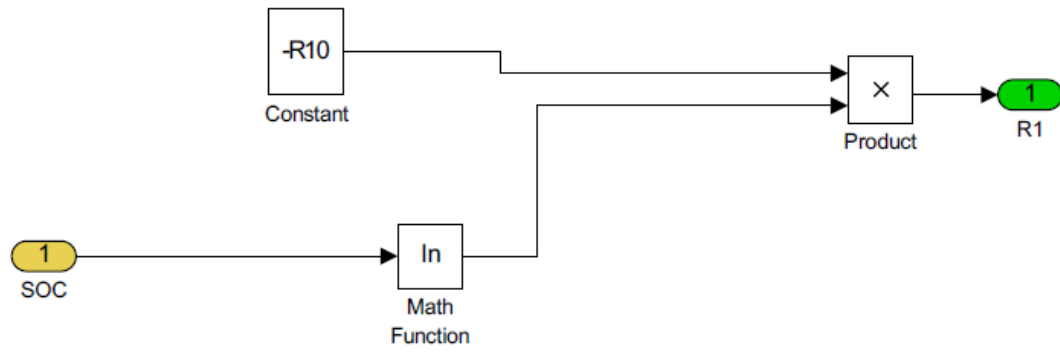
Battery Simulink Model











Battery m-file

```
%% Test data
cells_in_parallel =3;
cells_in_series=15*6;

%% assumed data
%Em block
theta = 31+273; %Temperature in Kelvin
Em0=301.102; % (volt) Sure from discharge test
v1=301; % (volt)
ke=.001; %(volt/degreeCelcius)

%R0 block
A0=-1.1976; %Constant
R00=0.0033; %Value of R0 at SOC=1

% R1 block
R10= 0.0025; %Constant in ohms

% C1 calculation
Taul= 10; %time lag approximately 10 sec

% R2 block % Insignificant for discharge currents
I_star=20;

% Charge and Capacity block
thetaf=-30+273; %sure from manufacturer
eps =0.001; % guessed, from a paper
kc =1.01; % guessed, from paper
kt=(1+(theta./thetaf)).^eps;
C0=69200; % No load capacity in Amp.sec equivalent to 19 Amp.hr
delt = 0.9; % guessed, from paper

% SOC
capacity_0= 20*3600;
SOC_0=.94;
OCV=[2.25
     3.2
     3.1934
     3.2196
     3.2416
     3.2571
     3.2688
     3.2803
     3.2941
     3.3109
     3.3526
     ]
```

```

%% Plots

figure(1)
    plot (bcm_soc./100, 'MarkerSize',2,'Marker','o','Color',[0 1 0],...
        'DisplayName',' Measured SOC ');
hold on
plot (SOC, 'MarkerSize',3,'LineWidth',2,'LineStyle','--',...
    'DisplayName','Simulated SOC',...
    'Color',[0 0 0]);
    xlabel('time (s)');...
    ylabel('SOC at I= 100Amps')
legend('Measured SOC','Simulated SOC')
grid on

figure (2)
subplot(2,1,1); plot
(bcm_vbat,'MarkerSize',3,'Marker','o','LineWidth',2,'Color',[0 1 0],...
    'DisplayName','Measured Voltage');
hold on
plot (vt, 'LineStyle','--','DisplayName','Simulated Voltage',...
    'Color',[0 0 0]);
    xlabel('time (s)');...
    ylabel('Output Voltage (v)')
grid on
legend('Measured Voltage','Simulated Voltage')
subplot(2,1,2); plot(I.signals.values, 'r'); xlabel('time (s)');
ylabel('Current (Amps)'); %title(' Constant Current Discharge')
grid on
legend('Current')

```

